Convective drying of yacón (Smallanthus sonchifolius) slices: A simple physical model including shrinkage

Bianca Cristine Marques, Artemio Plana-Fattori, Denis Flick, Carmen Cecilia Tadini

LWT

CONVECTIVE DRYING OF YACÓN (SMALLANTHUS SONCHIFOLIUS) SLICES: A SIMPLE PHYSICAL MODEL INCLUDING SHRINKAGE

--Manuscript Draft--

Manuscript Number:	LWT-D-21-04829R3
Article Type:	Research paper
Keywords:	Yacón; Convective drying; Drying kinetics; shrinkage behavior
Corresponding Author:	Artemio Plana-Fattori UMR Ingénierie Procédés Aliments, AgroParisTech, INRA, Université Paris-Saclay Paris, FRANCE
First Author:	BIANCA CRISTINE MARQUES
Order of Authors:	BIANCA CRISTINE MARQUES
	Artemio Plana-Fattori
	Denis Flick
	Carmen Cecilia Tadini
Abstract:	Yacón is a tuberous root from the Andean region, and a potential functional food because of the presence of fructo-oligossacharides (FOS). Due to its high moisture in natura , the product is prone to microbial degradation. The evolution of yacón cylindrical slices under convective drying is here studied from experimental work and theoretical considerations about bulk properties. The operation of a pilot-scale convective dryer allowed monitoring the moisture and dimensions of yacón slices. Evolution of moisture under temperature, and relative humidity, controlled conditions is described through a two-parameter drying kinetic model. A novel approach for estimating shrinkage effects is proposed, comparing measured dimensions with predictions based upon hypothetical shrinkage behaviors. The drying kinetics and the shrinkage approach are finally combined with the global energy balance for a single slice, in order to describe the evolution of surface temperature and other yacón slice properties along the drying period.

RÉPUBLIQUE FRANÇAISE
Liberté
Égalité
Fraternité

AgroParisTech
Talents for a sustainable planet

Bianca Cristine Marques
biancacm1@usp.br

Prof. Rakesh. K. SINGH
Editor-in-Chief
LWT - Food Science and Technology
São Paulo, January 10th 2022

Dear Prof. SINGH,

We are sending you a revised version of the manuscript that we have submitted in July 2021, co-authored by Artemio Plana-Fattori, Denis Flick, Carmen C. Tadini and myself. This version contains improvements, marked in red, motivated by the constructive criticism demonstrated by the Reviewers.

We thank you for considering our paper for publication.
Looking forward to hearing from you.

Yours sincerely,

Bianca Cristine Marques

On behalf of all authors

Responses to reviewer's remarks

We would like to thank the Editors and Reviewers for their suggestions, that were carefully reviewed. A new section in the manuscript (3.5) is marked in red. We kindly invite you to verify this new version, hoping that it is now appropriate for publishing at LWT. Thank you again for helping us improve our work.

HIGHLIGHTS

The evolution of yacón slices under convective drying was studied at pilot scale. 81

Experimental data were collected under controlled air temperature and humidity. 79

Moisture loss observations were approximated through a novel two-parameter model. 81

Shrinkage of yacón slices was described by a combination of hypothetical models. 80

The global energy balance allowed to predict surface water activity and temperature. 84

CONVECTIVE DRYING OF YACÓN (*SMALLANTHUS SONCHIFOLIUS*) SLICES: A SIMPLE PHYSICAL MODEL INCLUDING SHRINKAGE

Bianca Cristine Marques[1,2], Artemio Plana-Fattori[3]*, Denis Flick[3], Carmen Cecilia Tadini[1,2]

[1] Univ. de São Paulo, Escola Politécnica, Dept. of Chemical Eng., Main Campus, SP, Brazil.

[2] Universidade de São Paulo, FoRC/NAPAN– Food Research Center, Brazil

[3] Université Paris-Saclay, INRAE, AgroParisTech, UMR SayFood, 91300 Massy, France

(*) author corresponding address:

AgroParisTech, Dept. MMIP, 16 rue Claude Bernard, 75231 Paris CEDEX 5

E-mail: artemio.planafattori@agroparistech.fr

ABSTRACT

Yacón is a tuberous root from the Andean region, and a potential functional food because of the presence of fructo-oligossacharides (FOS). Due to its high moisture *in natura*, the product is prone to microbial degradation. The evolution of yacón cylindrical slices under convective drying is here studied from experimental work and theoretical considerations about bulk properties. The operation of a pilot-scale convective dryer allowed monitoring the moisture and dimensions of yacón slices. Evolution of moisture under temperature, and relative humidity, controlled conditions is described through a two-parameter drying kinetic model. A novel approach for estimating shrinkage effects is proposed, comparing measured dimensions with predictions based upon hypothetical shrinkage behaviors. The drying kinetics and the shrinkage approach are finally combined with the global energy balance for a single slice, in order to describe the evolution of surface temperature and other yacón slice properties along the drying period.

KEYWORDS

Yacón, convective drying, drying kinetics, shrinkage behavior

HIGHLIGHTS

The evolution of yacón slices under convective drying was studied at pilot scale. 81

Experimental data were collected under controlled air temperature and humidity. 79

Moisture loss observations were approximated through a novel two-parameter model. 81

Shrinkage of yacón slices was described by a combination of hypothetical models. 80

The global energy balance allowed to predict surface water activity and temperature. 84

1. Introduction

The mechanisms underlying the processing of food raw materials must be understood in order to: a) manufacture, in a reproducible manner, products for consumption, b) assess the influence of raw material variability, and c) provide insight into process optimization. Consumers are increasingly interested in the ingredients and processes associated with their food. “Clean labels” with recognizable ingredients, and as few preservatives as possible, are a trend in the food market (Asioli et al., 2017).

Here we focus on yacón (*Smallanthus sonchifolius*), a tuberous crop from the Asteraceae family, originally from the Andean region and nowadays cultivated worldwide. Its roots, described as succulent and mildly sweet, with a thin peel, can be eaten raw. While in the majority of storage roots the energy is stored as starch, in yacón it is stored as inulin and fructo-oligo-saccharides (FOS) instead. These compounds naturally exist in plants, but in concentrations usually lower than those in yacón roots. The human gastrointestinal tract does not have enzymes to digest these compounds, so they reach the gut microbiota practically intact (Grau and Rea, 1997; Hermann et al., 1999; Seminario et al., 2003; Lebeda et al., 2012). In other words, albeit sweet, they have a low caloric value for humans, making them an interesting option for diabetics. In addition, inulin and FOS are appreciated as effective and safe prebiotics (Fernandez et al., 2013) with claims of immunomodulatory effects (Watzl et al., 2005). Root flesh colors vary from white to yellow, orange, and purple, depending on the genotype (Hermann et al., 1999). Chemical characteristics, such as phenolic compounds and saccharides, may vary significantly between cultivars (Graefe et al., 2004; Khajehei et al., 2018b).

As a source of inulin and fructose, tuberous roots of yacón can be employed in the production of cold drinks and alcohol, dry crisps, jams and stewed fruits, sweeteners and some dairy products like yoghurt (Lebeda et al., 2012). A major portion of tuberous root biomass of yacón is composed of water (> 70% of fresh weight) (Lachman et al., 2003). Water activity is also high, leading to a short shelf life; partial hydrolysis of oligo-fructans can start within only a few days after harvest (Graefe et al., 2004). Drying is a convenient way to prepare yacón for storage, and the influence of drying conditions on the chemical composition of yacón samples has been investigated (Scher et al., 2009; Campos et al., 2016; Khajehei et al., 2018a; Salinas et al., 2018).

Several techniques have been applied to dehydrate yacón samples, including hot air convection drying (Scher et al., 2009), vacuum drying (Reis et al., 2012), freeze drying (Khajehei et al., 2018a), as well as hybrid techniques combining forced convection with osmotic dehydration (Perussello et al., 2013, 2014) or microwave heating (Shi et al., 2015). However, in drying yacón samples, none of these studies have controlled the air relative humidity. In other words, caution should be exercised in discussing these results: without control of relative humidity, ambient conditions may vary due to drying of the product. Such a control has been implemented in the drying of many foods, including apples (Assis et al., 2019; Sjoholm & Gekas, 1995) and potatoes (Hassini et al., 2007; Sandoval-Torres et al., 2017; Chua et al., 2000).

One of the most important physical changes undergone by food during drying is the reduction of its volume. Loss of water and heating cause stresses in the cellular structure of the food matrix, leading to changes in shape and decrease in dimension (Mayor and Sereno, 2004). The volume

reduction and shape modification of yacón samples under convective drying has been scarcely investigated (Bernstein and Noreña, 2014).

Different modeling approaches have been used for studying the evolution of fruits and other high-moisture-content food materials under convective drying (Castro et al., 2018). A complete thermo-hygro-mechanical model requires, in addition to thermal conductivity and water diffusivity, the knowledge of rheological parameters (Young's modulus, Poisson's coefficient, contraction coefficient due to water loss...). Especially under large deformation, the food material cannot be considered as purely elastic. Thermo-physical and mechanical parameters depend on temperature and moisture, and they are difficult to measure or estimate (Curcio and Aversa, 2014). In the case of yacón, these parameters were assessed under selected conditions (Blahovec et al., 2013; Perussello et al., 2013). The coupling of large deformation with heat and mass transfer phenomena in a single physical model constitutes a formidable challenge for yacón samples, because of the high water content in the fresh product and the significant volume reduction along the drying period. Determining the best approach for modelling requires, as a previous step, to choose the purpose and application of the model itself; simple models can fit the results properly, allowing the implementation of engineering aims (Castro et al., 2018).

This study concerns the convective drying of sets of cylindrical slices of yacón, after experiments carried out in a pilot-scale convective dryer; the operating conditions of air flow, temperature and relative humidity (RH) were controlled, which allowed stable ambient conditions. In accordance with literature (Bernstein and Norena, 2014), our preliminary tests have shown that the shrinkage

of yacón is by no means negligible. This result motivated us to design the set of experiments so we could measure the dimensions of selected samples throughout the drying period. Our first objective is thus to investigate the existence of relations between the ambient conditions and the modifications undergone by yacón cylinders during the drying period. The second objective is to study selected parameters associated with the convective drying of yacón samples, while considering a generalization of the shrinkage behavior identified from measurements.

2. Material and Methods

Tuberous roots of yacón used in this work were cultivated in Piedade, Sao Paulo, Brazil, and later purchased from a local market in two batches of 17 kg: one in July 2020, and the other in September 2020. The selected roots were free of injuries, and had a diameter higher than 40 mm. These roots had a tan surface and light-yellow flesh (Figs. 1a and 1b).

2.1. Vapor sorption isotherms

A VSA1055 vapor sorption analyzer (Decagon Devices, USA) was used to obtain vapor sorption isotherms. Yacón roots were cut into slices with 40 mm diameter and 3 mm thickness, and pre-dried in a forced circulation oven (model N480; Nova Ética, Brazil) for one hour. Isotherms were run using static (DVS) and dynamic (DDI) methods, from a_w = 0.9 to a_w = 0.1, then returning to a_w = 0.9. Experimental data were adjusted assuming the Guggenheim, Anderson and De Boer (GAB) model (van der Berg, 1984):

$$\frac{X_w}{X_{w,\text{mono}}} = \frac{CKa_w}{(1-Ka_w)(1+(C-1)Ka_w)} \quad , \qquad (1)$$

wherein X_w is the water content (kg/kg db); $X_{w,\text{mono}}$ is the monolayer water content (kg/kg db); C is the Guggenheim constant, K is the GAB correction factor, and a_w is the water activity in the food matrix.

2.2. Pretreatment

One setback in drying yacón is a browning effect caused by polyphenol oxidase (PPO), right after cutting the roots and exposing the enzyme to oxygen (Lachman et al., 2003; Yan et al., 1999); a blanching pretreatment is necessary in order to minimize this effect. Following Reis et al. (2012), a citric acid pretreatment was used: firstly, using molds, approximately 500 g of yacón roots were cut into cylindrical slices (40 mm diameter and 7 mm height) (Fig. 1b); secondly, the slices were submerged in 500 mL of a 2 g/L aqueous citric acid (purity 95 g/100g; Tate & Lyle, Brazil) solution for 3 min; finally, the slices were placed on absorbent paper before use.

Before each experiment, three slices were randomly picked to have their moisture determined. The dry-matter mass was determined according to AOAC method 926.12 (1996); results ranged from 9 to 11% of fresh weight.

2.3. Drying experiments at pilot-scale

Drying experiments were performed in a LM-ES20 drying oven (Labmaq, Brazil). This oven has a chamber with four removable trays, each placed upon a scale, which allows real-time recording of weight. It is also possible to control the temperature and relative humidity at the air-drying inlet. On the roof of the oven, there is a 10 cm quartz window, equipped with a S6D stereo-microscope (Leica, Germany); images of a single sample can be acquired during the whole drying period.

For each drying experiment, 42 yacón slices (360 g total) were placed on the top tray, and dried until no variation in weight was recorded for fifteen minutes. The following ambient conditions were studied: [T_{air} = 50 °C, RH = 20 %]; [60 °C, 20 %]; [50 °C, 30 %] and [60 °C, 30 %], all at an airspeed of 4 m/s. Three full drying experiments were conducted under each of these four ambient conditions.

2.4. Dimensions

To determine the slice diameter over time, images acquired along with the drying experiments with the stereo-microscope setup were analyzed through an image processing software (version LAS6; Leica Microsystems Applications, Switzerland). In the case of the sample height, in a separate experiment, three yacón slices were dried in the same pilot unit. The height was measured using a micrometer (model 103-137; Mitutoyo, Brazil), in a point near the border and also at the center. The whole procedure was repeated many times along the drying period, for each of the four controlled ambient conditions. This method assumes that the cylindrical format was maintained during the drying process. Although irregularities appeared on the samples and

159 the shape became somewhat disturbed, the circular shape was roughly retained. It is possible to
160 consistently identify a diameter and a height along the drying period.

161

162 **3. Macroscopic modeling**

163 In this work, the average properties are estimated from measurements collected over ensembles
164 of many cylindrical slices of yacón slices (Fig.1b).

165

166 *3.1. Shrinkage*

167 Shrinkage during drying takes place simultaneously with moisture diffusion, and thus may affect
168 the moisture removal rate; volume changes and deformation depend on several factors including
169 sample geometry, dehydration method and drying conditions (Moreira et al., 2000). Experimental
170 work has demonstrated that shrinkage behavior encountered during drying of real food products
171 is neither ideally three-dimensional, nor unidimensional (Sjoholm and Gekas, 1995).

172 In the scope of this study, the sample volume was calculated by adding the volumes of the dry
173 matter and the water:

174 $$V = m_{dm}\left(\frac{1}{\rho_{dm}} + \frac{X_w}{\rho_w}\right) \quad (2)$$

175 $$V_0 = m_{dm}\left(\frac{1}{\rho_{dm}} + \frac{X_{w0}}{\rho_w}\right), \quad (3)$$

wherein V is the volume (m^3); V_0 is the initial volume before drying (m^3); m_{dm} is the mass of the dry-matter mass (kg); ρ_{dm} is the density of the dry-matter mass (kg m^{-3}); ρ_w is the water density (kg m^{-3}); and X_{w0} is the initial water content of the product (kg water/kg dry matter), on dry basis, before drying.

The water content was expressed in its normalized form (X_w^*):

$$X_w^* = \frac{X_w}{X_{w0}} \quad . \tag{4}$$

Dimensionless volume (V^*) and surface (S^*) of the sample can be computed from measured dimensions and water content, as:

$$V^* = \frac{1+\left(\frac{\rho_{dm}}{\rho_w}\right) X_{w0}\, X_w^*}{1+\left(\frac{\rho_{dm}}{\rho_w}\right) X_{w0}} \tag{5}$$

or, alternatively:

$$V^* = \frac{(\pi\, D^2\, H/4)}{(\pi\, D_0^2\, H_0/4)} = H^*(D^*)^2 \tag{6}$$

$$S^* = \frac{(2\,\pi\, D^2/4) + \pi\, D\, H}{(2\,\pi\, D_0^2/4) + \pi\, D_0\, H_0} = D^*\left(\frac{D^* + 2\, H^*\, H_0/D_0}{1+2\, H_0/D_0}\right) \quad . \tag{7}$$

Simplified models, based on different assumptions, may describe the shrinkage behavior of the slices. For all the approaches, the slice surface area can be expressed in the form of Eq. 7.

A first approach, named as “vertical model”, based on measurements performed at the beginning of drying, assumes that the shrinkage in the radial direction is negligible compared to the vertical one:

$$H^*_{\text{vert}} = \frac{V}{V_0}\,;\; D^*_{\text{vert}} = 1 \quad . \tag{8}$$

A second approach assumes isotropic shrinkage. This approach resembles the linear, uniform model described by Mayor and Sereno (2004) for a cube, but to predict height and diameter directly, instead of the area:

$$H^*_{\text{iso}} = D^*_{\text{iso}} = \left(\frac{V}{V_0}\right)^{\frac{1}{3}} \quad . \tag{9}$$

Finally, after seeing that the measurements did not match any of these approaches, we looked for intermediate behaviors allowing a satisfying match with the experimental results. Hereafter, Eq. 8 and 9 are combined. The dimensionless height assuming combined shrinkage is expressed as:

$$H^*_{\text{comb}} = (H^*_{\text{iso}})^b (H^*_{\text{vert}})^{(1-b)}\,; \quad D^*_{\text{comb}} = (D^*_{\text{iso}})^b \quad , \tag{10}$$

wherein b is the moisture-dependent weighting parameter.

The first approach (D^* = 1) fits the measurements at the beginning of drying (Fig. 4). Yet progressively (as X^*_w decreases) the diameter of the slices also decreases. This is why we propose increasing the relative importance of the isotropic approach along with the drying process. An approach using a similar principle was proposed by Suzuki et al. (1976); it was described by Mayor and Sereno (2004) as a “semi-core drying model”. Our approach, however, involves a

208 different geometry and does not require as many parameters. At the end ($X_w^* \approx 0$), equal
209 importance is given to the purely-vertical and isotropic approaches, resulting in:

210 $$b = \frac{1}{2}(1 - X_w^*) \quad . \tag{11}$$

211 Assuming such a combined shrinkage behavior, the dimensionless total surface (S_{comb}^*) is
212 calculated through Eq. 7, using the dimensionless height and diameter from Eq. 10.

213

214 *3.2. Drying kinetics*

215 Semi-theoretical models have been derived by simplifying general series solutions of Fick's
216 second law; they are thus valid within the air temperature, relative humidity, flow velocity and
217 moisture content range for which they were developed; further, these models require less
218 time compared to theoretical thin-layer models and do not need assumptions of geometry of a
219 typical food, its mass diffusivity or conductivity. Many of these semi-theoretical drying models
220 have been compared in the literature (e.g., Panchariya et al., 2002); some of them are shown in
221 Table 2.

222 The evolution of the overall moisture in the product under drying can be described through the
223 moisture ratio:

224 $$MR = \frac{X_w - X_{we}}{X_{w0} - X_{we}} \ , \tag{12}$$

where X_{we} is the water content in equilibrium, estimated from vapor sorption isotherms. In the scope of this study, the following two-parameter model was adjusted to the drying kinetics data:

$$MR = exp(-k_1\, t - (k_2\, t)^2)\ ; \tag{13}$$

the inverse value of parameter k_1 can be called characteristic drying time. Equation 13 can be seen as an extension of the Lewis (1921) drying model, which considers the first term in the exponential only.

The time derivative of Eq. 13 can be expressed as:

$$\frac{dMR}{dt} = (-k_1 - 2\, t\, k_2^2)\big(exp(-t\, k_1 - t^2\, k_2^2)\big)\ . \tag{14}$$

When drying starts ($t = 0$), it follows $dMR/dt = -k_1$. By defining the dimensionless time $t* = t\, k_1$ (at any time), the evaporative water loss per dimensionless area can be expressed as:

$$\frac{dMR}{dt^* S^*} = -MR\left(1 + \frac{2\, t\, k_2^2}{k_1}\right)\frac{1}{S^*_{\text{comb}}}\ . \tag{15}$$

3.3 Heat transfer coefficient between yacón samples and surrounding air

3.3.1. Experimental method

The heat transfer coefficient is a key parameter for assessing the importance of exchanges between the product under consideration and its surroundings. Looking for its experimental determination, a well-known material of regular geometry was heated in the same conditions as

the yacón slices were dried. Two aluminum cylinders, each containing a hole (1 mm radius, 10 mm height), were used in this experiment. Their properties are summarized in Table 1.

For each experiment, two calibrated thermocouples were used: one inserted in the aluminum cylinder, filled with thermal paste (MasterGel Maker, Cooler Master, Taiwan) and the other exposed to the air, as shown in Fig. 1d. The measurements (carried out at T_{air} = 60 ° C, RH = 20% and speed of 4 m/s) were carried out until the recorded temperatures became constant, or almost. Data acquisition was performed using Labview software (National Instruments, USA).

The heat transfer coefficient was determined using a two-step approach, based on the lumped capacitance method (Incropera et al., 2007, pp.256-263). The energy balance takes the form:

$$-\square A_S \quad (T - T_{\text{air}}) = m\, C_P \frac{dT}{dt} \ , \tag{16}$$

wherein h is the heat transfer coefficient ($Wm^{-2}\,K^{-1}$), A_S is the surface area exposed to airflow (m^2), T is the product temperature at any time (ºC), T_{air} is the air temperature (ºC), m is the mass (kg) and C_P the specific heat ($J\,kg^{-1}\,K^{-1}$) of the product, and t is the time (s).

Observations revealed that the air temperature did not reach perfect steady state evolution. Hence, in the first step, Eq. 16 was integrated numerically using an in-house source code written in Python 3.7 language. The second step involved the minimization of the sum squared differences of residuals between measured and predicted temperatures, these latter obtained after assuming selected h values. Such minimization has considered the Nelder-Mead method.

260

261 *3.3.2. Global energy balance method*

262 Assuming that all the incoming heat is translated into evaporation at the surface temperature, it

263 follows (McCabe et al., 2014, p.807):

264 $$-\frac{dm_w}{dt\,S} = -\frac{d(m_{dm}\,X_w)}{dt\,S} = \frac{\square}{L_v}\left(T_{air} - T_{surf}\right) \rightarrow\ -\frac{dX_w}{dt} = \frac{\square\ S\,(T_{air}-T_{surf})}{m_{dm}\,L_v}\ , \qquad (17)$$

265 wherein m_w is the mass of water in the sample (kg).

266 The time derivative of Eq. 12 is:

267 $$\frac{dMR}{dt} = \frac{1}{X_{w0}-X_{we}}\frac{dX_w}{dt}\ \rightarrow\ -\frac{dX_w}{dt} = -(X_{w0} - X_{we})\frac{dMR}{dt}\ . \qquad (18)$$

268 Combining Eqs. 17 and 18, the time derivative of Eq. 12 can be expressed in terms of

269 temperature values in ambient air and at the product surface:

270 $$-(X_{w0} - X_{we})\frac{dMR}{dt} = \frac{\square S\,(T_{air}-T_{surf})}{m_{dm}\,L_v} \rightarrow\ \frac{dMR}{dt} = -\frac{\square\ S\,(T_{air}-T_{surf})}{m_{dm}\,L_v\,(X_{w0}-X_{we})}\ . \qquad (19)$$

271 When drying starts, $dMR/dt = -k_1$; hence, at this moment:

272 $$\square = k_1\frac{m_{dm}\,L_v\,(X_{w0}-X_{we})}{S_0\,(T_{air}-T_{wb})}\ , \qquad (20)$$

273 assuming that $T_{surf} = T_{wb}$ at $t = 0$.

274 Application of Eq. 20 requires the mass of dry-matter in the sample. The mass density of dry-

275 matter in our samples was estimated to be about 1590 kg/m^3. Firstly, data provided by Hermann

et al. (1999) about nine accessions of fresh yacón allowed us to assess the averaged weight fraction of selected pure components: 0.374 % for proteins, 0.0235 % for fat, 10.8 % for carbohydrates, 0.361 % for fibers, and 0.505 % for ash. These values were considered in applying the Choi and Oikos (1986)'s approach for estimating the mass density of dry-matter of yacón samples at the temperature 40 °C. This temperature value is between the temperature prevailing in the product when drying starts (about 20 °C) and the ambient surrounding temperature (60 °C during the drying period).

3.4. Global energy balances

The evaporative water loss can be expressed by a global energy balance assuming that all the heat entering the sample causes water evaporation. Equation 17 can be applied if the variation of sensible heat can be neglected. This is approximately the case except at the beginning of drying, when the sample temperature increases toward the wet-bulb one if free water is available on the surface.

The initial water content is very high ($X_{w0} \approx 11$ kg/kg d.b.); therefore, it can be assumed that the water activity is close to 1 and that the product surface temperature is close to the wet-bulb one ($T_{surf} = T_{wb}$). Thus, combining Eqs. 19 and 20, we obtain:

$$\frac{T_{\text{air}}-T_{\text{surf}}}{T_{\text{air}}-T_{wb}} = \frac{(dMR/dt)/S}{(dMR/dt)|_{t=0}/S_0} = \frac{1}{1-X_{we}/X_{w0}}\frac{S}{S_0}\frac{dX_w^*}{k_1\,dt} = \frac{1}{(1-X_{we}/X_{w0})\,S^*}\frac{dX_w^*}{dt^*} \quad , \qquad (21)$$

where:

$$\frac{dMR}{dt} = \frac{1}{1-X_{we}/X_{w0}} \frac{dX_w^*}{dt} \quad . \tag{22}$$

The water mass balance can also express the evaporative water loss:

$$\frac{-dm_w}{dt\ S} = k(c_{w,\text{surf}} - c_{w,\text{air}}) \quad , \tag{23}$$

wherein k is the mass transfer coefficient (m s^{-1}), $c_{w,surf}$ is the concentration of water vapor in the air on the surface of the product (kg m^{-3}), and $c_{w,air}$ is the water vapor concentration in the surrounding air (kg m^{-3}).

Eq. 23 can be written in terms of dimensionless water content evolution:

$$\frac{dX_w}{dt} = \frac{k\ S\ (c_{w,\text{surf}} - c_{w,\text{air}})}{m_{dm}} \quad . \tag{24}$$

Comparing Eqs. 17 and 24, and rearranging water vapor concentration values in the place of temperatures, we can estimate the water activity at the slice surface as:

$$\frac{c_{w,\text{air}} - a_w\ c_{w,\text{sat}}(T_{\text{surf}})}{c_{w,\text{air}} - c_{w,\text{sat}}(T_{wb})} = \frac{T_{\text{air}} - T_{\text{surf}}}{T_{\text{air}} - T_{wb}} \quad . \tag{25}$$

The saturated water vapor concentration is obtained from the ideal gas law and Clausius-Clapeyron relation (Çengel et al., 2015):

$$c_{w,\text{sat}}(T_{\text{surf}}) = \frac{P_{\text{sat}}^{T_{\text{surf}}} M_w}{R\ T_{\text{surf}}} \quad , \tag{26}$$

wherein $P_{\text{sat}}^{T_{\text{surf}}}$ is the saturated vapor pressure at a temperature T and R is the gas constant (8.314 J K^{-1} mol^{-1}). The water concentration at the surface was estimated through a GAB model for parameters $X_{w,\text{mono}}$, C and K resulting from desorption measurements.

In summary:

a) pilot-scale drying experiments allowed the monitoring of water content X_w and slice dimensions D and H under controlled ambient conditions;

b) for each of these ambient conditions, desorption models enabled us to estimate the equilibrium moisture X_{we} value;

c) with the latter, the evolution of the moisture ratio MR was represented through the two-parameter drying kinetics, providing the initial drying rate;

d) monitoring the slice dimensions allowed us to identify a mean shrinkage behavior, and hence to predict the slice surface evolution;

e) finally, the availability of water content and surface evolutions allowed us to estimate the surface temperature and the surface water activity (Eq. 25).

4. Results

4.1. Vapor sorption isotherms

Vapor sorption isotherms for yacón (Fig. 2) can be characterized as being type III, which are common for products with a high quantity of soluble sugars (Rizvi, 2005; Al-Muhtaseb et al.,

328 2002). It can be observed that there was little difference between static and dynamic methods,
329 and between tested temperatures, and no visible hysteresis.

330 GAB model parameters, adjusted to the isotherms, are shown in Table 3. $X_{w,mono}$ is an estimation
331 of the monolayer water content; under this value, food materials tend to be very stable (Roos,
332 2008). However, packaging conditions are important to delay the re-absorption of water.

333

334 *4.2. Drying kinetics*

335 Figure 3 shows the evolution of the moisture ratio of ensembles of yacón slices, under the
336 ambient conditions here considered. Table 4 summarizes the results obtained after applying
337 Eq.13, and other models available in the literature, to the data obtained from each of the three
338 tests carried out under each of the four controlled conditions; averaged values were compared
339 using ANOVA and a post-hoc Tukey test ($p<0.05$), carried out using Statgraphics software
340 (version 19 Centurion; Statgraphics Technologies, USA). A number of findings emerge from
341 these results.

342 a) Under the ambient conditions considered, the application of Eq. 13 allows a smaller root-
343 mean-square-error (RMSE) than other two-parameters models available in the literature.
344 We argue that the Eq. 13 constitutes a good candidate for engineering aims.
345 b) The influence of ambient conditions on the values estimated for model parameters is here
346 preliminary assessed, because only three runs were conducted under each ambient
347 condition. Excepting the Page model, the influence of both air temperature and relative

348 humidity on parameter k_1 seems significant. This finding is consistent with the physical
349 meaning of this parameter; it is directly related to the initial drying rate, and its value
350 increases with the driving force $(T_{air} - T_{wb})$. The influence of air temperature on the
351 second parameter of Eq. 13, of Modified Page, and of Henderson-Pabis models seems
352 significant.

353 c) It is quite hard to compare model parameters estimated from our experimental data with
354 those provided by other authors. Air flow and temperature conditions were different, and
355 there was no control of air relative humidity, allowing ambient conditions which were
356 perhaps unsteady. An additional difficulty comes from the diversity of yacón; Hermann et
357 al. (1999) studied nine different cultivars of yacón, and they differed in appearance and
358 composition: the dry matter content alone could range from 98 to 136 g/kg, suggesting
359 that the drying kinetics can vary from a cultivar to another. Reis et al. (2012) reported the
360 time of purchase, but not the location; Shi et al (2013) purchased their roots in China; and
361 Lisboa et al. (2018) reported a purchase in Brazil, but not the season. None of these
362 studies reported the variety used, nor any descriptors, there thus being a possibility that
363 those authors studied different varieties of yacón.

364

365 *4.3. Shrinkage*

366 Left-hand side of Fig. 4 summarizes all the available experimental data, in terms of
367 dimensionless values for the slice height (Fig. 4a) and diameter (4c) as function of the
368 dimensionless water content. Triplicates were conducted. Right-hand side of Fig. 4 compares

369 measurements with similar predicted by hypothetical shrinkage behaviors; in the case of slice
370 height, triangles indicate averaged values; in the case of slice diameter, measurements do not
371 correspond to same water content and then averaging was not possible.

372 Figures 4b and 4d compare measurements and hypothetical shrinkage behaviors: purely-vertical,
373 isotropic and combined models for both diameter and height (Eqs. 8, 9, and 10, respectively). Up
374 to X_w^* = 0.2, the slice diameter remained at more than 90 % of the initial value; the proposed
375 vertical model is thus a more realistic approach than the isotropic one. Afterward, there was a
376 drastic reduction in diameter. Figures 4b and 4d suggest that the combined behavior, which mixes
377 the vertical and the isotropic approaches, describes the slice shrinkage better than the others.
378 Looking for a consistent approach for predicting the shrinkage of yacón slices under convective
379 drying, the combined approach was considered.

380

381 *4.4. Heat transfer coefficient between yacón samples and surrounding air*

382 A first estimation of the heat transfer coefficient relevant to our problem comes from
383 experimental work with aluminum slices (sub-section 3.3.1). The results obtained were h = 41 W
384 $m^{-2}\,K^{-1}$ for the 35 mm cylinder and 53 W $m^{-2}\,K^{-1}$ for the 20 mm one.

385 The consistency of these findings can be discussed using the correlation method. Taking in
386 account uniform heat flux conditions over a flat plate under laminar flow, it can be shown that the
387 averaged Nusselt, Reynolds and Prandtl numbers are related through the correlation
388 $\mathrm{Nu} = \alpha\, Re^{\beta}\, Pr^{\gamma}$ (Incropera et al., 2007, p.410). In our case, this expression can be

389 rewritten in order to indicate the heat transfer coefficient as a function of the cylinder diameter:
390 $h = \delta D^{\beta-1}$ wherein $\beta - 1 < 0$. According to this rationale, the heat transfer coefficient should
391 increase during drying while the yacón dimension reduces. Hence, it is consistent to reach h = 41
392 W m^{-2} K^{-1} for experimental data collected with a 35 mm aluminum cylinder and 53 W m^{-2} K^{-1}
393 with a 20 mm one.

394 A second estimation of the heat transfer coefficient between yacón samples and surrounding air
395 can be obtained by applying the expression $h = \delta D^{\beta-1}$ to our experimental conditions. Given
396 the airflow and temperature conditions above the surface of the cylinders, we can estimate the
397 Reynolds number to be about 10000 for a 40 mm cylinder (yacón sample, before any drying),
398 hence lower than the critical value for the laminar-turbulent transition for external flow
399 (Incropera et al., 2007, p.361). For these conditions, that correlation yields a heat transfer
400 convective coefficient 39 $Wm^{-2}K^{-1}$ for a 40 mm cylinder. Note that the aforementioned
401 correlation and the experimental values correspond to a physical problem bounded by an
402 adiabatic surface below the cylinder.

403 Finally, the heat transfer coefficient between yacón samples and surrounding air was estimated
404 by applying Eq. 20, i.e. by considering the initial evaporative rate results. The value obtained
405 (32 W m^{-2} K^{-1}) implicitly takes into account the global influence of a number of factors affecting
406 the heat and mass transfer relevant to the problem, including: a) the fact that not one but an
407 ensemble of 42 yacón slices were simultaneously processed in the convective dryer pilot unit; b)
408 the role played by the heterogeneous exposure of slices to air flow, c) the influence of thermal

409 radiation interaction of slices with the metallic walls of the dryer, and d) the fact that there was a
410 metallic holed surface below the yacón samples, allowing a complex situation of heat and mass
411 transfer.

412

413 *4.5. Predictions of temperature and water activity on the surface*

414 Experimental results displayed in Fig. 3 suggest that the most reproducible condition was T_{air} =
415 60 °C, RH = 20 %. We hypothesize that better reproducibility is due to the humidity stabilization
416 system of the convective dryer pilot unit. On the one hand, when the thermo-hygrometer detects a
417 value of RH below the set point, the control system of the drying oven sprays water into the
418 airflow and as it is not preheated, it could destabilize the temperature in the oven. On the other
419 hand, when humidity is above the set point, the air passes through a refrigerating system, where
420 water condensates and is removed, and the air must be heated again before re-entering the oven.
421 At the highest temperature (60 °C), the air has a higher ability to hold water from the samples
422 without going over the set point; and, in the lowest RH, there is no need to add moisture to the
423 air at the end of the drying process, to keep a high RH, leading to less destabilization. In the
424 forthcoming last steps of this study, we restrict our attention to measurements and predictions
425 corresponding to the ambient condition T_{air} = 60 °C, RH = 20%.

426 The identification of a suitable shrinkage behavior allows to predict the slice surface, which is
427 exposed to surrounding air along the drying period (S*). Representing the drying kinetics
428 through the two-parameter model allows to predict, also along the whole period, the drying rate

429 $\frac{dX_w^*}{dt^*}$. Figure 5a shows the predictions for the slice surface (Eq. 7) and for the drying rate (Eqs. 14
430 and 22) as a function of the dimensionless water content. The influence of the total surface
431 decrease on the drying rate $\frac{dX_w^*}{dt^* S^*}$ is noticeable, but only partially explains the drop in this drying
432 rate. Figure 5b exhibits the same variables as function of time, which can be compared with the
433 classical drying curves (Mujumdar, 2006). Note that $\frac{dX_w^*}{dt^* S^*}$ does not present a constant rate
434 period, indicating that some drying limitation due to the resistance of water migration from the
435 center to the surface of the product may exist.

436

437 The availability of key quantities S^* and $\frac{dX_w^*}{dt^*}$ enables to estimate surface-averaged values for the
438 temperature T, the water activity a_w and the water content X_w at the slice surface along the
439 drying period. Figure 5c shows that, as expected, the predicted water content at the surface
440 decreases more rapidly than the volume-averaged value for the sample. Note that GAB models do
441 not accurately represent the sorption phenomena at very high (a_w > 0.93) water activities (Basu et
442 al., 2006); hence, the predicted water content at the surface tends to be underestimated at the
443 beginning of drying.

444 Finally, Fig. 5d displays the water activity and temperature at the product surface. In the case of
445 the water activity, the departure from pre-drying conditions is immediate, contrarily to
446 experimental results (see for instance Figure 1 of Bernstein and Norena, 2014). In the case of
447 temperature, firstly the surface-averaged temperature increases almost instantaneously from the

initial product temperature (20 °C) up to the wet bulb temperature (about 35 °C); later on, this temperature increases from the wet-bulb temperature up to the air temperature along the remaining drying period. It would be interesting to assess the reliability of these predictions, for instance using a non-invasive technique, such as an infrared thermometer.

4.6. A remark about moisture diffusivity

Shi et al. (2013) and Lisboa et al. (2018) used the Crank (1975) solutions to the Fick's laws in order to estimate the effective moisture diffusion coefficient for yacón samples. These solutions, however, assume that the shrinkage is negligible. Results in Section 4.3 demonstrate that this is not the case for yacón samples as tested here. The infinite slab and the finite cylinder models, common in the literature, revealed to be unreliable fits for the experimental drying data displayed in Fig. 3. In the case of the infinite slab model, estimated moisture diffusivity was 4.0 10^{-10} m^2 s^{-1} at 50 °C, and 7.4 10^{-10} m^2 s^{-1} at 60 °C, and a root mean square error of 0.033 and 0.060 in MR units, respectively. However, the fitted curve tended to underestimate the moisture ratio in the beginning of the drying period, and to overestimate it after two hours of drying. Anyway, given the drastic differences in sample's water content, dimensions and temperature between the beginning and the end of the drying process, it is likely incorrect to attribute a single, constant moisture diffusivity value over the whole drying process.

5. Conclusions and Recommendations

The study focused on the evolution of yacón samples having a particular shape and being exposed to convective drying under controlled ambient conditions (mean air velocity of 4 m/s, air temperature of 50 and 60 °C, air relative humidity of 20 and 30 %). The slice dimensions were measured along the drying period, as an original contribution to the classical monitoring of moisture loss. A dataset including triplicates of samples' water content, diameter and height allowed us to study the evolution of yacón slices while including the influence of shrinkage. Surface-averaged temperature and water activity tendencies were estimated from standard assumptions about heat and mass transfer phenomena, providing a useful insight about the drying evolution of a complex food product. The following conclusions were reached.

i) The diameter of yacón slices decreased to about 60-70 % of initial value after 6 hours of drying without a clear dependence on the ambient condition under consideration, i.e. following nearly the same decreasing tendency. The height of yacón slices was more difficult to determine, because irregularities which progressively appeared on upper and lower surfaces along the drying period. Available results indicated a reduction to 5-30 % of initial value after 6 hours of drying, with the decreasing tendency being a little different under relative humidity of 20 and 30 %.

ii) In the case of yacón slices as tested here, a combined shrinkage behavior was identified: it mixes purely-vertical (no diameter modification) with isotropic shrinkage (that progressively operates inside the product matrix). Such a novel approach was later applied in predicting firstly

488 the slice total surface as a function of the water content inside it, and secondly the evolution of
489 selected properties at the yacón slice surface along the drying period.

490

491 iii) The application of two-parameter model for representing the drying kinetics (Eq. 13) allowed
492 us to estimate the heat transfer coefficient between yacón samples and surrounding ambient
493 conditions. The value obtained (32 W m^{-2} K^{-1}) implicitly includes the global influence of a
494 number of factors affecting the heat and mass transfer relevant to the problem. Two other
495 approaches (experimental work with aluminum cylinders, and correlation involving
496 dimensionless numbers) provided independent estimates of this transfer coefficient, and the
497 whole set of results seems consistent.

498

499 iv) Evolutions of moisture ratio from measurements were poorly represented by the semi-
500 theoretical model proposed by Lewis (1921), towards the ending of the drying period (Fig. 3).
501 That classical model was proposed under a number of assumptions including negligible
502 shrinkage, which constitutes a hypothesis unacceptable for yacón samples. The inclusion of a
503 quadratic term in Eq. 13 apparently mitigates this problem (Fig. 3). We argue that the Eq. 13
504 constitutes a good candidate for engineering aims, in which the whole drying period must be
505 represented as properly as possible.

506 The crucial issue of this study was to follow the dimensions of the sample throughout the drying
507 period. Our pioneering strategy could be improved, for example by measuring the height of the
508 sample using an optical detection method.

509 The suitability of our approach to the design and optimization of the process as well as of the
510 final product could be explored. As a preliminary step, testing this approach should consider
511 wider ranges of ambient conditions (airflow, temperature and relative humidity) and including
512 different varieties of yacón and other raw food products. Much work remains to be done in order
513 to clarify the relationship between shrinkage and moisture loss.

514

515 **ACKNOWLEDGMENTS**

516 The authors have received grants from the São Paulo Research Foundation (FAPESP), grants
517 2018/21327-1 and 2019/21832-0; from the Coordination for the Improvement of Higher
518 Education Personnel - Brazil (CAPES) - Finance Code 001; and from the National Council for
519 Scientific and Technological Development (CNPq), grant 306414/2017-1. We would like to
520 thank AgroParistech and UMR Sayfood for receiving the first author for a one-year research
521 internship abroad; and Emmanuel Bernuau, for his valuable help to calculate the heat transfer
522 coefficient.

523 Declarations of interest: none.

524 **REFERENCES**

525 Al-Muhtaseb, A. H., McMinn, W. A. M., & Magee, T. R. A. (2002). Moisture sorption isotherm
526 characteristics of food products: A review. *Food Bioproducts Process*, *80*, 118–128.
527 https://doi.org/10.1205/09603080252938753.

528 AOAC. (1996). Moisture and volatile matter in oils and fats (926.12-1926). In *Official Methods*
529 *of Analysis, 15th ed.*, Association of Official Analytical Chemists, Washington, USA.

530 Asioli, D., Aschemann-Witzel, J., Caputo, V., Vecchio, R., Annunziata, A., Næs, T., & Varela, P.
531 (2017). Making sense of the "clean label" trends: A review of consumer food choice behavior
532 and discussion of industry implications. *Food Research International, 99*, 58–71.
533 https://doi.org/10.1016/j.foodres.2017.07.022.

534 Assis, F. R., Rodrigues, L. G. G., Tribuzi, G., de Souza, P. G., Carciofi, B. A. M., & Laurindo, J.
535 B. (2019). Fortified apple (*Malus* spp., var. Fuji) snacks by vacuum impregnation of calcium
536 lactate and convective drying. *LWT – Food Science and Technology*, *113*, 108298.
537 https://doi.org/10.1016/j.lwt.2019.108298.

538 Basu, S., Shivhare, U. S., & Mujumdar, A. S. (2006). Models for sorption isotherms for foods: A
539 review. *Drying Technology, 24*, 917–930. https://doi.org/10.1080/07373930600775979.

540 * Bernstein, A., & Noreña, C. P. Z. (2014). Study of thermodynamic, structural, and quality
541 properties of yacón (*Smallanthus sonchifolius*) during drying. *Food and Bioprocess Technology,*
542 *7*, 148-160. https://link.springer.com/article/10.1007/s11947-012-1027-y.

543 Blahovec, J., Lahodova, M., Kindl, M., & Fernandez, E. C. (2013). DMA thermal analysis of
544 yacón tuberous roots. *International Agrophysics, 27*, 479-483. https://doi.org/10.2478/intag-
545 2013-0018.

Campos, D., Aguilar-Galvez, A., & Pedreschi, R. (2016). Stability of fructooligosaccharides, sugars and colour of yacón (*Smallanthus sonchifolius*) roots during blanching and drying. *International Journal of Food Science and Technology, 51*, 1177-1185. https://doi.org/10.1111/ijfs.13074.

Çengel, Y., Boles, M., & Kanoğlu, M. (2015). Thermodynamic property relations. In: *Thermodynamics an engineering approach*. Mc McGraw-Hill.

Castro, A. M., Mayorga, E. Y., & Moreno, F. L. (2018). Mathematical modelling of convective drying of fruits: A review. *Journal of Food Engineering, 223*, 152-167. https://doi.org/ 10.1016/j.jfoodeng.2017.12.012.

Choi, Y., & Okos, M. R. (1986). Effects of temperature and composition on the thermal properties of foods. In M. Le Mageur, & P. Jelen (Eds.), *Food Engineering and Process Applications* (pp. 93-101). Elsevier Applied Science.

Chua, K. J., Mujumdar, A. S., Chou, S. K., Hawlader, M. N. A., & Ho, J. C. (2000). Convective drying of banana, guava and potato pieces : Effect of cyclical variations of air temperature on drying kinetics and color change. *Drying Technology, 18*, 907–936. https://doi.org/10.1080/07373930008917744.

Crank, J. (1975). *The Mathematics of Diffusion* (2nd ed.). Oxford University Press.

563 Curcio, S., & Aversa, M. (2014). Influence of shrinkage on convective drying of fresh
564 vegetables: A theoretical model. *Journal of Food Engineering, 123*, 36-49.
565 http://dx.doi.org/10.1016/j.jfoodeng.2013.09.014.

566 Fernández, E. C., Rajchl, A., Lachman, J., Čížková, H., Kvasnička, F., Kotíková, Z., & Voldřich,
567 M. (2013). Impact of yacón landraces cultivated in the Czech Republic and their ploidy on the
568 short- and long-chain fructo-oligosaccharides content in tuberous roots. *LWT - Food Science and*
569 *Technology*, *54*, 80–86. https://doi.org/10.1016/j.lwt.2013.05.013.

570 Graefe, S., Hermann, M., Manrique, I., Golombek, S., & Buerkert, A. (2004). Effects of post-
571 harvest treatments on the carbohydrate composition of yacon roots in the Peruvian Andes. *Field*
572 *Crops Research*, *86*, 157–165. https://doi.org/10.1016/j.fcr.2003.08.003.

573 Grau, A., & Rea, J. (1997). Yacón, Smallanthus sonchifolius (Poepp. et Endl.) H. Robinson. In:
574 M. Hermann & J. Heller (Eds.), *Promoting the conservation and use of underutilized and*
575 *neglected crops, #21, Andean roots and tubers: Ahipa, arracacha, maca and yacón* (pp. 199-
576 242). International Plant Genetic Resources Institute.

577 Hassini, L., Azzouz, S., Peczalski, R., & Belghith, A. (2007). Estimation of potato moisture
578 diffusivity from convective drying kinetics with correction for shrinkage. *Journal of food*
579 *engineering.* 79, 47–56. https://doi.org/10.1016/j.jfoodeng.2006.01.025.

580 * Hermann, M., Freire, I., & Pazos, C. (1999). Compositional diversity of the yacón storage root.
581 In *Andean Roots and Tuber Crops* (pp. 425-432). International Potato Center Program Report
582 1997-1998.

583 Incropera, F. P., Witt, D. P., Bergman, T. L., Lavine, A. S. (2007). *Fundamentals of heat and*
584 *mass transfer* (6th ed.). Wiley.

585 Khajehei, F., Hartung, J., & Graeff-Hönninger, S. (2018a). Total phenolic content and antioxidant
586 activity of yacón (*Smallanthus sonchifolius Poepp. and Endl.*) chips: Effect of cultivar, pre-
587 treatment, and drying. *Agriculture, 8,* 183. https://doi.org/10.3390/agriculture8120183.

588 Khajehei, F., Merkt, N., Claupein, W., & Graeff-Hönninger, S. (2018b). Yacón (*Smallanthus*
589 *sonchifolius Poepp. & Endl.*) as a novel source of health promoting compounds: Antioxidant
590 activity, phytochemicals and sugar content in flesh, peel, and whole tubers of seven cultivars.
591 *Molecules, 23,* 278. http://dx.doi.org/10.3390/ molecules23020278.

592 Lachman, J., Fernández, E. C., & Orsák, M. (2003). Yacón [*Smallanthus sonchifolia (Poepp. et*
593 *Endl.) H. Robinson*] chemical composition and use: A review. *Plant, Soil and Environment, 49,*
594 283–290. https://doi.org/10.17221/4126-PSE.

595 Lebeda, A., Doležalová, I., Fernández, E., & Viehmannová, I. (2012). Yacón (*Asteraceae*;
596 *Smallanthus sonchifolius*). In R. J. Singh (Ed.), *Genetic Resources, Chromosome Engineering,*
597 *and Crop Improvement. Volume 6: Medicinal Plants* (pp. 641-702). CRC Press.

598 * Lewis, W. K. (1921). The rate of drying of solid materials. *Industrial & Engineering Chemistry*
599 *Research, 13,* 427–432. https://doi.org/10.1021/ie50137a021.

Lisboa, C., Gomes, J., Figueirêdo, R., Queiroz, A., Diógenes, A., & de Melo, J. (2018). Effective diffusivity in yacón potato cylinders during drying. *Revista Brasileira de Engenharia Agrícola e Ambiental*, *22*, 564–569. https://doi.org/10.1590/1807-1929/agriambi.v22n8p564-569.

* Mayor, L., & Sereno, A. M. (2004). Modelling shrinkage during convective drying of food materials: A review. *Journal of Food Engineering*, *61*, 373-386. http://dx.doi.org/10.1016/S0260-8774(03)00144-4.

McCabe, W., Smith, J., & Harriott, P. (2014). Drying of solids. In: *Unit operations of chemical engineering* (7th ed.). Mc Graw Hill.

Moreira, R., Figueiredo, A., & Sereno, A. (2000). Shrinkage of apple disks during drying by warm air convection and freeze drying. *Drying Technology*, *18*, 279-294. https://doi.org/10.1080/07373930008917704.

Mujumdar, A. S. (2006). Principles, Classification, and Selection of Dryers. In *Handbook of Industrial Drying*. Taylor and Francis.

Panchariya, P. C., Popovic, D., & Sharma, A. L. (2002). Thin-layer modelling of black tea drying process. *Journal of Food Engineering*, *52*, 349-357. https://doi.org/10.1016/S0260-8774(01)00126-1.

Perussello, C. A., Mariani, V. C., Masson, M. L., & Castilhos, F. (2013). Determination of thermophysical properties of yacón (*Smallanthus sonchifolius*) to be used in a finite element

simulation. *International Journal of Heat and Mass Transfer, 67*, 1163-1169. http://dx.doi.org/10.1016/j.ijheatmasstransfer.2013.09.004.

Perussello, C. A., Kumar, C., De Castilhos, F., & Karim, M. A. (2014). Heat and mass transfer modeling of the osmo-convective drying of yacón roots (*Smallanthus sonchifolius*). *Applied Thermal Engineering, 63*, 23–32. https://doi.org/10.1016/j.applthermaleng.2013.10.020.

Perry, R. H., & Green, D. W. (1997). Section 2: Physical and chemical data. In *Perry's Engineers' Handbook* (7th ed.). Mc Graw-Hill.

Rizvi, S. H. (2005). Thermodynamic Properties of Foods in Dehydration. In *Engineering Properties of Foods* (3rd ed.). Boca Raton: CRC Press.

Reis, F. R., Lenzi, M. K., de Muñiz, G. I. B., Nisgoski, S., & Masson, M. L. (2012). Vacuum drying kinetics of yacón (*Smallanthus sonchifolius*) and the effect of process conditions on fractal dimension and rehydration capacity. *Drying Technology, 30*, 13–19. https://doi.org/10.1080/07373937.2011.611307.

Roos, Y.H. (2008). Water Activity and Glass Transition. In *Water Activity in Foods: Fundamentals and Applications*, (1st ed.). Blackwell Publishing Professional.

* Scher, C. F., Rios, A., & Noreña, C. (2009). Hot air drying of yacón (*Smallanthus sonchifolius*) and its effect on sugar concentrations. *International Journal of Food Science and Technology, 44*, 2169–2175. https://doi.org/10.1111/j.1365-2621.2009.02056.x.

636 Salinas, J. G., Alvarado, J. A., Bergenståhl, B., & Tornberg, E. (2018). The influence of
637 convection drying on the physicochemical properties of yacón (*Smallanthus sonchifolius*). *Heat*
638 *and Mass Transfer, 54*, 2951-2961. https://doi.org/10.1007/s00231-018-2334-2.

639 Sandoval-Torres, S., Tovilla-Morales, A. S., & Hernández-Bautista, E. (2017). Dimensionless
640 modeling for convective drying of tuberous crop (Solanum tuberosum) by considering shrinkage.
641 *Journal of Food Engineering, 214*, 147–157. https://doi.org/10.1016/j.jfoodeng.2017.06.014.

642 Seminario, J., Valderrama, M., & Manrique, I. (2003). *El Yacón : Fundamentos para el*
643 *Aprovechamiento de un Recurso Promisorio*. Lima (Peru): Centro Internacional de la Papa (CIP),
644 Universidad Nacional de Cajamarca, Agencia Suiza para el Desarollo y la Cooperacion
645 (COSUDE).

646 Shi, Q., Zheng, Y., & Zhao, Y. (2013). Mathematical modeling on thin-layer heat pump drying of
647 yacón (*Smallanthus sonchifolius*) slices. *Energy Conversion and Management, 71*, 208–216.
648 https://doi.org/10.1016/j.enconman.2013.03.032.

649 Shi, Q., Zheng, Y., & Zhao, Y. (2015). Thermal transition and state diagram of yacón dried by
650 combined heat pump and microwave method. *Journal of Thermal Analysis and Calorimetry, 119*,
651 727–735. https://doi.org/10.1007/s10973-014-4198-0.

652 Sjoholm, I., & Gekas, V. (1995). Apple shrinkage upon drying. *Journal of Food Engineering, 25*,
653 123-130. https://doi.org/10.1016/0260-8774(94)00001-P.

Suzuki, K., Kubota, K., Hasegawa, T., & Hosaka, H. (1976). Shrinkage in dehydration of root vegetables. *Journal of Food Science, 41*, 1189–1193. https://doi.org/10.1111/j.1365-2621.1976.tb14414.x.

van den Berg, C. (1984). Description of water activity of foods for engineering purposes by means of the G.A.B. model of sorption. In B. M. McKenna (Ed.), *Engineering and Food (Proceedings of the Third International Congress on Engineering and Food held between 26 and 28 September 1983 at Trinity College, Dublin, Ireland)* (vol. 1, pp. 311-321). London (UK): Elsevier Applied Science Publishers.

Watzl, B., Girrbach, S., & Roller, M. (2005). Inulin, oligofructose and immunomodulation. *British Journal of Nutrition, 93*, S49. https://doi.org/10.1079/BJN20041357.

Yan, X., Suzuki, M., Ohnishi-Kameyama, M., Sada, Y., Nakanishi, T., & Nagata, T. (1999). Extraction and identification of antioxidants in the roots of yacón (*Smallanthus sonchifolius*). *Journal of Agricultural and Food Chemistry, 47*, 4711–4713. https://doi.org/10.1021/jf981305o.

Figure captions

Fig. 1. Yacón roots: (a) in *natura*, still with their tan-colored peel; (b) being cut for the drying experiments, with their light-yellow flesh visible; (c) dried, with the perforated tray on the background; and (d) experimental arrangement to estimate the heat transfer coefficient.

Fig. 2. Sorption isotherms (desorption and adsorption) for yacón obtained at two temperatures through the methods DDI and DVS, in comparison with the adjusted GAB model for DVS test at 60 °C.

675 **Fig. 3.** Moisture ratio of yacón slices, expressed in function of time (a) at T_{air} = 50 °C and *RH* =
676 30 %; (b) at 60 °C and 30 %; (c) at 50 °C and 20 %; (d) at 60 °C and 20 %, compared to the
677 drying kinetics model proposed in this work, and to the Lewis (1921) model.

678 **Fig. 4.** Dimensionless height and diameter of yacón slices as a function of dimensionless water
679 content along with the drying: (a) all height measurements performed under four ambient
680 conditions; (b) height measurement averages, compared to predictions reached after assuming
681 different hypothetical behaviors for slice shrinkage; (c) as in (a) but for the diameter; (d) as in (b)
682 but for the diameter. In the case of the vertical shrinkage assumption, the dimensionless diameter
683 equals unity (Eq.8).

684 **Fig. 5.** Predictions about the drying behavior of yacón slices. In display (a), the dimensionless
685 surface S^* comes from Eq.7, the drying rate dX_w^*/dt^* comes from Eq.22 with dMR/dt from
686 Eq.14. In display (b), same as (a) but as a function of time. In display (c), slice-averaged and
687 surface moisture as a function of time. In display (d), surface temperature from Eq.21 and water
688 activity from Eq.25 as a function of time.

689

690

691 **Justifying key references**

692 Please see below our remarks regarding our five key references, sorted by year of publication. They
693 are indicated by a star in the reference section of our manuscript.

694

695 1) Lewis, W. K. - 1921 - The rate of drying the solid materials. The Journal of Industrial and
696 Engineering Chemistry, 13: 427-432. https://doi.org/10.1021/ ie50137a021.

> This founding article allowed us to understand the basic rationale of semi-theoretical drying kinetics models. The Lewis' model can be presented as

$$d\,MR / dt = -k\,t,$$

where symbols are explained in our Nomenclature. In the present study we propose an extension of the Lewis' model:

$$d\,MR / dt = -k_1\,t - k_2\,t^2.$$

The second-order term might incorporate, implicitly, the bulk influence of complex phenomena in drying the solid matrix (including shrinkage, which was neglected by Lewis). Results suggest that this extended model fits better our experimental data than the Lewis' one.

2) Hermann, M., Freire, I., Pazos, C. - 1999 - Compositional diversity of the yacón storage root. In « Andean Roots and Tuber Crops », International Potato Center Program Report 1997-1998, Lima (Peru), pp.425-432.

> Very few articles compare the physico-chemical composition (fibers, proteins, carbohydrates, etc) of different yacón varieties. This article allowed us to estimate the dry-matter mass density associated with an averaged composition over nine yacón cultivars.

714 3) Mayor, L., Sereno, A. M. - 2004 - Modelling shrinkage during convective drying of food
715 materials: A review. Journal of Food Engineering, 61: 373-386. https://doi.org/10.1016/S0260-
716 8774(03)00144-4.

717 > This classical reference inspired us in our analysis of experimental data, more precisely in
718 comparing measurements of dimensions of yacón slices along the drying period with predictions
719 from hypothetical shrinkage behaviors.

720

721

4) Scher, C. F., Rios, A. O., Norena, C. P. Z. - 2009 - Hot air drying of yacón (Smallanthus sonchifolius) and its effect on sugar concentrations. International Journal of Food Science and Technology, 44 : 2169-2175. https://doi.org/10.1111/j.1365-2621.2009.02056.

> This dense article discusses the influence of drying conditions on yacón sugar contents and water activity, among other relevant characteristics. The design of our own experimental work was, in some extent, inspired by this article.

5) Bernstein, A., Norena, C. P. Z. - 2014 – Study of thermodynamic, structural, and quality properties of yacón (Smallanthus sonchifolius) during drying. Food and Bioprocess Technology, 7: 148-160. https://link.springer.com/article/ 10.1007/s11947-012-1027-y.

> This very interesting article provided us insight about yacón samples: their volume reduction along some hours of drying, their micro-structure after different treatments, and water activity at selected temperatures.

CONVECTIVE DRYING OF YACÓN (*SMALLANTHUS SONCHIFOLIUS*) SLICES: A SIMPLE PHYSICAL MODEL INCLUDING SHRINKAGE

Bianca Cristine Marques[1,2], Artemio Plana-Fattori[3]*, Denis Flick[3], Carmen Cecilia Tadini[1,2]

[1] Univ. de São Paulo, Escola Politécnica, Dept. of Chemical Eng., Main Campus, SP, Brazil.

[2] Universidade de São Paulo, FoRC/NAPAN– Food Research Center, Brazil

[3] Université Paris-Saclay, INRAE, AgroParisTech, UMR SayFood, 91300 Massy, France

(*) author corresponding address:

AgroParisTech, Dept. MMIP, 16 rue Claude Bernard, 75231 Paris CEDEX 5

E-mail: artemio.planafattori@agroparistech.fr

ABSTRACT

Yacón is a tuberous root from the Andean region, and a potential functional food because of the presence of fructo-oligosaccharides (FOS). Due to its high moisture *in natura*, the product is prone to microbial degradation. The evolution of yacón cylindrical slices under convective drying is here studied from experimental work and theoretical considerations about bulk properties. The operation of a pilot-scale convective dryer allowed monitoring the moisture and dimensions of yacón slices. Evolution of moisture under temperature, and relative humidity, controlled conditions is described through a two-parameter drying kinetic model. A novel approach for estimating shrinkage effects is proposed, comparing measured dimensions with predictions based upon hypothetical shrinkage behaviors. The drying kinetics and the shrinkage approach are finally combined with the global energy balance for a single slice, in order to describe the evolution of surface temperature and other yacón slice properties along the drying period.

KEYWORDS

Yacón, convective drying, drying kinetics, shrinkage behavior

HIGHLIGHTS

The evolution of yacón slices under convective drying was studied at pilot scale. 81

Experimental data were collected under controlled air temperature and humidity. 79

Moisture loss observations were approximated through a novel two-parameter model. 81

Shrinkage of yacón slices was described by a combination of hypothetical models. 80

The global energy balance allowed to predict surface water activity and temperature. 84

1. Introduction

The mechanisms underlying the processing of food raw materials must be understood in order to: a) manufacture, in a reproducible manner, products for consumption, b) assess the influence of raw material variability and c) provide insight into process optimization. Consumers are increasingly interested in the ingredients and processes associated with their food. “Clean labels” with recognizable ingredients, and as few preservatives as possible, are a trend in the food market (Asioli et al., 2017).

Here we focus on yacón (*Smallanthus sonchifolius*), a tuberous crop from the Asteraceae family, originally from the Andean region and nowadays cultivated worldwide. Its roots, described as succulent and mildly sweet, with a thin peel, can be eaten raw. While in the majority of storage roots the energy is stored as starch, in yacón it is stored as inulin and fructo-oligosaccharides (FOS) instead. These compounds naturally exist in plants, but in concentrations usually lower than those in yacón roots. The human gastrointestinal tract does not have enzymes to digest these compounds, so they reach the gut microbiota practically intact (Grau and Rea, 1997; Hermann et al., 1999; Seminario et al., 2003; Lebeda et al., 2012). In other words, albeit sweet, they have a low caloric value for humans, making them an interesting option for diabetics. In addition, inulin and FOS are appreciated as effective and safe prebiotics (Fernandez et al., 2013) with claims of immunomodulatory effects (Watzl et al., 2005). Root flesh colors vary from white to yellow, orange, and purple, depending on the genotype (Hermann et al., 1999). Chemical characteristics, such as phenolic compounds and saccharides, may vary significantly between cultivars (Graefe et al., 2004; Khajehei et al., 2018b).

As a source of inulin and fructose, tuberous roots of yacón can be employed in the production of cold drinks and alcohol, dry crisps, jams and stewed fruits, sweeteners and some dairy products like yogurt (Lebeda et al., 2012). A major portion of the tuberous root biomass of

yacón is composed of water (>0.7 g/g w.b.) (Lachman et al., 2003). Water activity is also high, leading to a short shelf-life; partial hydrolysis of oligo-fructans can start within only a few days after harvest (Graefe et al., 2004). Drying is a convenient way to prepare yacón for storage, and the influence of drying conditions on the chemical composition of yacón samples has been investigated (Scher et al., 2009; Campos et al., 2016; Khajehei et al., 2018a; Salinas et al., 2018).

Several techniques have been applied to dehydrate yacón samples, including hot air convection drying (Scher et al., 2009), vacuum drying (Reis et al., 2012), freeze-drying (Khajehei et al., 2018a), as well as hybrid techniques combining forced convection with osmotic dehydration (Perussello et al., 2013, 2014) or microwave heating (Shi et al., 2015). However, in drying yacón samples, none of these studies have controlled the air relative humidity. In other words, caution should be exercised in discussing these results: without control of relative humidity, ambient conditions may vary due to the drying of the product. Such control has been implemented in the drying of many foods, including apples (Assis et al., 2019; Sjoholm & Gekas, 1995) and potatoes (Hassini et al., 2007; Sandoval-Torres et al., 2017; Chua et al., 2000).

One of the most important physical changes undergone by food during drying is the reduction of its volume. Loss of water and heating cause stresses in the cellular structure of the food matrix, leading to changes in shape and a decrease in dimension (Mayor and Sereno, 2004). The volume reduction and shape modification of yacón samples under convective drying has been scarcely investigated (Bernstein and Noreña, 2014).

Different modeling approaches have been used for studying the evolution of fruits and other high-moisture-content food materials under convective drying (Castro et al., 2018). A complete thermo-hygro-mechanical model requires, in addition to thermal conductivity and water diffusivity, the knowledge of rheological parameters (Young's modulus, Poisson's

coefficient, contraction coefficient due to water loss...). Especially under large deformation, the food material cannot be considered purely elastic. Thermo-physical and mechanical parameters depend on temperature and moisture, and they are difficult to measure or estimate (Curcio and Aversa, 2014). In the case of yacón, these parameters were assessed under selected conditions (Blahovec et al., 2013; Perussello et al., 2013). The coupling of large deformation with heat and mass transfer phenomena in a single physical model constitutes a formidable challenge for yacón samples, because of the high water content *in natura* and the significant volume reduction along the drying period. Determining the best approach for modeling requires, as a previous step, to choose the purpose and application of the model itself; simple models can fit the results properly, allowing the implementation of engineering aims (Castro et al., 2018).

This study concerns the convective drying of sets of cylindrical slices of yacón, after experiments carried out in a pilot-scale convective dryer; the operating conditions of airflow, temperature and relative humidity (RH) were controlled, which allowed stable ambient conditions. In accordance with the literature (Bernstein and Norena, 2014), our preliminary tests have shown that the shrinkage of yacón is by no means negligible. This result motivated us to design the set of experiments so we could measure the dimensions of selected samples throughout the drying period. Our first objective is thus to investigate the existence of relations between the ambient conditions and the modifications undergone by yacón cylinders during the drying period. The second objective is to study selected parameters associated with the convective drying of yacón samples while considering a generalization of the shrinkage behavior identified from measurements.

2. Material and Methods

Tuberous roots of yacón used in this work were cultivated in Piedade, Sao Paulo, Brazil, and later purchased from a local market in two batches of 17 kg: one in July 2020, and the other in

September 2020. The selected roots were free of injuries and had a diameter higher than 40 mm. These roots had a tan surface and light-yellow flesh (Figs. 1a and 1b).

2.1. Vapor sorption isotherms

A VSA1055 vapor sorption analyzer (Decagon Devices, USA) was used to obtain vapor sorption isotherms. Yacón roots were cut into slices with 40 mm diameter and 3 mm thickness, and pre-dried in a forced circulation oven (model N480; Nova Ética, Brazil) for one hour. Isotherms were run using static (DVS) and dynamic (DDI) methods, from a_w = 0.9 to a_w = 0.1, then returning to a_w = 0.9. Experimental data were adjusted assuming the Guggenheim, Anderson and De Boer (GAB) model (van der Berg, 1984):

$$\frac{X_w}{X_{w,mono}} = \frac{CKa_w}{(1\text{-}Ka_w)(1+(C\text{-}1)Ka_w)} \quad (1)$$

Wherein X_w is the water content (kg/kg db); $X_{w,\text{mono}}$ is the monolayer water content (kg/kg db); C is the Guggenheim constant, K is the GAB correction factor, and a_w is the water activity in the food matrix.

2.2. Pretreatment

One setback in drying yacón is a browning effect caused by polyphenol oxidase (PPO), right after cutting the roots and exposing the enzyme to oxygen (Lachman et al., 2003; Yan et al., 1999); a blanching pretreatment is necessary in order to minimize this effect. Following Reis et al. (2012), a citric acid pretreatment was used: firstly, approximately 500 g of yacón roots were cut into cylindrical slices (40 mm diameter and 7 mm height) (Fig. 1b), using circular cutters; secondly, the slices were submerged in 500 mL of a 2 g/L aqueous citric acid (purity 95 g/100g; Tate & Lyle, Brazil) solution for 3 min; finally, the slices were placed on absorbent paper before use.

Before each experiment, three slices were randomly picked to have their moisture determined. The dry-matter mass was determined according to AOAC method 926.12 (1996); results ranged from 0.09 to 0.11 g/g w.b.

2.3. Drying experiments at pilot-scale

Drying experiments were performed in a LM-ES20 drying oven (Labmaq, Brazil). This oven has a chamber with four removable trays, each placed upon a scale, which allows real-time recording of weight. It is also possible to control the temperature and relative humidity at the air-drying inlet. On the roof of the oven, there is a 10 cm quartz window, equipped with a S6D stereo-microscope (Leica, Germany); images of a single sample can be acquired during the whole drying period.

For each drying experiment, 42 yacón slices (360 g total) were placed on the top tray and dried until no variation in weight was recorded for fifteen minutes. The following drying air conditions were studied: [T_{air} = 50 °C, RH = 20 %]; [60 °C, 20 %]; [50 °C, 30 %] and [60 °C, 30 %], all at an airspeed of 4 m/s. Three full drying experiments were conducted under each of these four conditions.

2.4. Dimensions

To determine the slice diameter over time, images acquired along with the drying experiments with the stereo-microscope setup were analyzed through an image processing software (version LAS6; Leica Microsystems Applications, Switzerland). In the case of the sample height, in a separate experiment, three yacón slices were dried in the same pilot unit. The height was measured using a micrometer (model 103-137; Mitutoyo, Brazil), at a point near the border and also at the center. The whole procedure was repeated many times along the drying period, for each of the four controlled ambient conditions. This method assumes that the cylindrical format was maintained during the drying process. Although irregularities appeared on the samples and the shape became somewhat disturbed, the circular shape was

157 roughly retained. It is possible to consistently identify a diameter and a height along the
158 drying period.

159 **3. Macroscopic modeling**

160 In this work, the average properties are estimated from measurements collected over
161 ensembles of many cylindrical slices of yacón slices (Fig.1b).

162 *3.1. Shrinkage*

163 Shrinkage during drying takes place simultaneously with moisture diffusion, and thus may
164 affect the moisture removal rate; volume changes and deformation depend on several factors
165 including sample geometry, dehydration method and drying conditions (Moreira et al., 2000).
166 Experimental work has demonstrated that shrinkage behavior encountered during drying of
167 real food products is neither ideally three-dimensional nor unidimensional (Sjoholm and
168 Gekas, 1995).

169 In the scope of this study, the sample volume was calculated by adding the volumes of the dry
170 matter and the water:

171 $$V = m_{dm}\left(\frac{1}{\rho_{dm}} + \frac{X_w}{\rho_w}\right) \quad (2)$$

172 $$V_0 = m_{dm}\left(\frac{1}{\rho_{dm}} + \frac{X_{w0}}{\rho_w}\right) \quad (3)$$

173 wherein V is the volume (m^3); V_0 is the initial volume before drying (m^3); m_{dm} is the mass of
174 the dry-matter mass (kg); ρ_{dm} is the density of the dry-matter mass (kg m^{-3}); ρ_w is the water
175 density (kg m^{-3}); and X_{w0} is the initial water content of the product (kg water/kg dry matter),
176 on a dry basis, before drying.

177 The water content was expressed in its normalized form (X_w^*):

178 $$X_w^* = \frac{X_w}{X_{w0}} \quad (4)$$

179 Dimensionless volume (V^*) and surface (S^*) of the sample can be computed from measured
180 dimensions and water content, as:

181 $$V^* = \frac{1 + \left(\frac{\rho_{dm}}{\rho_w}\right) X_{w0} X_w^*}{1 + \left(\frac{\rho_{dm}}{\rho_w}\right) X_{w0}} \quad (5)$$

182 or, alternatively:

183 $$V^* = \frac{\left(\pi D^2 H/4\right)}{\left(\pi D_0^2 H_0/4\right)} = H^* (D^*)^2 \quad (6)$$

184 $$S^* = \frac{\left(2\pi \frac{D^2}{4}\right) + \pi D H}{\left(2\pi \frac{D_0^2}{4}\right) + \pi D_0 H_0} = D^* \left(\frac{D^* + 2 H^* \frac{H_0}{D_0}}{1 + \frac{2 H_0}{D_0}} \right) \quad (7)$$

185 Simplified models, based on different assumptions, may describe the shrinkage behavior of
186 the slices. For all the approaches, the slice surface area can be expressed in the form of Eq. 7.
187 A first approach, named as "vertical model", based on measurements performed at the
188 beginning of drying, assumes that the shrinkage in the radial direction is negligible compared
189 to the vertical one:

190 $$H_{vert}^* = \frac{V}{V_0}; \; D_{vert}^* = 1 \quad (8)$$

191 A second approach assumes isotropic shrinkage. This approach resembles the linear, uniform
192 model described by Mayor and Sereno (2004) for a cube, but to predict height and diameter
193 directly, instead of the area:

194 $$H_{iso}^* = D_{iso}^* = \left(\frac{V}{V_0}\right)^{\frac{1}{3}} \quad (9)$$

195 Finally, after seeing that the measurements did not match any of these approaches, we looked
196 for intermediate behaviors allowing a satisfying match with the experimental results.

Hereafter, Eq. 8 and 9 are combined. The dimensionless height assuming combined shrinkage is expressed as:

$$H^*_{comb}=(H^*_{iso})^b (H^*_{vert})^{(1-b)} \; ; \quad D^*_{comb}=(D^*_{iso})^b \tag{10}$$

wherein b is the moisture-dependent weighting parameter.

The first approach ($D^*= 1$) fits the measurements at the beginning of drying (Fig. 4). Yet progressively (as X^*_w decreases) the diameter of the slices also decreases. This is why we propose increasing the relative importance of the isotropic approach along with the drying process. An approach using a similar principle was proposed by Suzuki et al. (1976); it was described by Mayor and Sereno (2004) as a "semi-core drying model". Our approach, however, involves a different geometry and does not require as many parameters. At the end ($X^*_w \approx 0$), equal importance is given to the purely-vertical and isotropic approaches, resulting in:

$$b=\frac{1}{2}\left(1-X^*_w\right) \tag{11}$$

Assuming such a combined shrinkage behavior, the dimensionless total surface (S^*_{comb}) is calculated through Eq. 7, using the dimensionless height and diameter from Eq. 10.

3.2. Drying kinetics

Semi-theoretical models have been derived by simplifying general series solutions of Fick's second law; they are thus valid within the air temperature, relative humidity, flow velocity and moisture content range for which they were developed; further, these models require less time compared to theoretical thin-layer models and do not need assumptions of the geometry of typical food, its mass diffusivity or conductivity. Many of these semi-theoretical drying models have been compared in the literature (e.g., Panchariya et al., 2002); some of them are shown in Table 2.

The evolution of the overall moisture in the product under drying can be described through the moisture ratio:

$$MR = \frac{X_w - X_{we}}{X_{w0} - X_{we}} \quad (12)$$

where X_{we} is the water content in equilibrium, estimated from vapor sorption isotherms. In the scope of this study, the following two-parameter model was adjusted to the drying kinetics data:

$$MR = \exp(-k_1 t - (k_2 t)^2) \quad (13)$$

the inverse value of parameter k_1 can be called characteristic drying time. Equation 13 can be seen as an extension of the Lewis (1921) drying model, which considers the first term in the exponential only.

The time derivative of Eq. 13 can be expressed as:

$$\frac{dMR}{dt} = \left(-k_1 - 2 t k_2^2\right)\left(\exp\left(-t k_1 - t^2 k_2^2\right)\right) \quad (14)$$

When drying starts (t = 0), it follows $dMR/dt = -k_1$. By defining the dimensionless time $t^* = t k_1$ (at any time), the evaporative water loss per dimensionless area can be expressed as:

$$\frac{dMR}{dt^* S^*} = -MR\left(1 + \frac{2 t k_2^2}{k_1}\right)\frac{1}{S^*_{comb}} \quad (15)$$

3.3 Heat transfer coefficient between yacón samples and surrounding air

3.3.1. Experimental method

The heat transfer coefficient is a key parameter for assessing the importance of exchanges between the product under consideration and its surroundings. Looking for its experimental determination, a well-known material of regular geometry was heated in the same conditions as the yacón slices were dried. Two aluminum cylinders, each containing a hole (1 mm radius, 10 mm height), were used in this experiment. Their properties are summarized in Table 1.

For each experiment, two calibrated thermocouples were used: one inserted in the aluminum cylinder, filled with thermal paste (MasterGel Maker, Cooler Master, Taiwan) and the other exposed to the air, as shown in Fig. 1d. The measurements (carried out at T_{air} = 60 ° C, RH = 20% and speed of 4 m/s) were carried out until the recorded temperatures became constant, or almost. Data acquisition was performed using Labview software (National Instruments, USA).

The heat transfer coefficient was determined using a two-step approach, based on the lumped capacitance method (Incropera et al., 2007). The energy balance takes the form:

$$-h\,A_S(T-T_{air}) = m\,C_P\frac{dT}{dt} \tag{16}$$

wherein h is the heat transfer coefficient ($Wm^{-2}\,K^{-1}$), A_S is the surface area exposed to airflow (m^2), T is the product temperature at any time (ºC), T_{air} is the air temperature (ºC), m is the mass (kg) and C_P the specific heat ($J\,kg^{-1}\,K^{-1}$) of the product, and t is the time (s).

Observations revealed that the air temperature did not reach perfect steady-state evolution. Hence, in the first step, Eq. 16 was integrated numerically using an in-house source code written in Python 3.7 language. The second step involved the minimization of the sum squared differences of residuals between measured and predicted temperatures, these latter were obtained after assuming selected h values. Such minimization has been considered the Nelder-Mead method.

3.3.2. Global energy balance method

Assuming that all the incoming heat is translated into evaporation at the surface temperature, it follows (McCabe et al., 2014, p.807):

$$-\frac{dm_w}{dt\,S} = -\frac{d(m_{dm}\,X_w)}{dt\,S} = \frac{h}{L_v}\left(T_{air}-T_{surf}\right) \rightarrow -\frac{dX_w}{dt} = \frac{h\,S\left(T_{air}-T_{surf}\right)}{m_{dm}\,L_v} \tag{17}$$

wherein m_w is the mass of water in the sample (kg).

The time derivative of Eq. 12 is:

$$\frac{dMR}{dt} = \frac{1}{X_{w0}\text{-}X_{we}} \frac{dX_w}{dt} \rightarrow -\frac{dX_w}{dt} = -(X_{w0}\text{-}X_{we}) \frac{dMR}{dt} \quad (18)$$

Combining Eqs. 17 and 18, the time derivative of Eq. 12 can be expressed in terms of temperature values in ambient air and at the product surface:

$$-(X_{w0}\text{-}X_{we}) \frac{dMR}{dt} = \frac{hS\left(T_{air}\text{-}T_{surf}\right)}{m_{dm}\, L_v} \rightarrow \frac{dMR}{dt} = -\frac{h\, S\left(T_{air}\text{-}T_{surf}\right)}{m_{dm}\, L_v\, (X_{w0}\text{-}X_{we})} \quad (19)$$

When drying starts, $dMR/dt = -k_1$; hence, at this moment:

$$h = k_1 \frac{m_{dm}\, L_v\, (X_{w0}\text{-}X_{we})}{S_0\, (T_{air}\text{-}T_{wb})} \quad (20)$$

assuming that $T_{surf} = T_{wb}$ at $t = 0$.

Application of Eq. 20 requires the mass of dry matter in the sample. The mass density of dry matter in the samples used in this work was estimated to be about 1590 kg/m^3. Firstly, we used data provided by Hermann et al. (1999) about nine accessions of fresh yacón, including the averaged weight fraction of selected pure components, as an estimation for the composition of the samples used in this work: 0.37 % for proteins, 0.024 % for fat, 11 % for carbohydrates, 0.36 % for fibers, and 0.51 % for ash. These values were considered in applying the Choi and Oikos (1986)'s approach for estimating the mass density of dry-matter of yacón samples at the temperature of 40 °C. This temperature value is between the temperature prevailing in the product when drying starts (about 20 °C) and the ambient surrounding temperature (60 °C during the drying period).

3.4. Global energy balances

The evaporative water loss can be expressed by a global energy balance assuming that all the heat entering the sample causes water evaporation. Equation 17 can be applied if the variation of sensible heat can be neglected. This is approximately the case except at the beginning of

drying when the sample temperature increases toward the wet-bulb one if free water is available on the surface.

The initial water content is very high ($X_{w0} \approx 11$ kg/kg d.b.); therefore, it can be assumed that the water activity is close to 1 and that the product surface temperature is close to the wet-bulb one ($T_{surf} = T_{wb}$). Thus, combining Eqs. 19 and 20, we obtain:

$$\frac{T_{air}\text{-}T_{surf}}{T_{air}\text{-}T_{wb}} = \frac{(dMR/dt)/S}{(dMR/dt)|_{t=0}/S_0} = \frac{1}{1\text{-}X_{we}/X_{w0}} \frac{S}{S_0} \frac{dX_w^*}{k_1\, dt} = \frac{1}{(1\text{-}X_{we}/X_{w0})\, S^*} \frac{dX_w^*}{dt^*} \tag{21}$$

wherein:

$$\frac{dMR}{dt} = \frac{dX_w^*}{dt} \tag{22}$$

The water mass balance can also express the evaporative water loss:

$$\frac{\text{-}dm_w}{dt\, S} = k\left(c_{w,surf}\text{-}c_{w,air}\right) \tag{23}$$

wherein k is the mass transfer coefficient (m s^{-1}), $c_{w,surf}$ is the concentration of water vapor in the air on the surface of the product (kg m^{-3}), and $c_{w,air}$ is the water vapor concentration in the surrounding air (kg m^{-3}).

$$\frac{dX_w}{dt} = \frac{k\, S\, (c_{w,surf}\text{-}c_{w,air})}{m_{dm}} \tag{24}$$

Comparing Eqs. 17 and 24, and rearranging water vapor concentration values in the place of temperatures, we can estimate the water activity at the slice surface as:

$$\frac{c_{w,air}\text{-}a_w\, c_{w,sat}\left(T_{surf}\right)}{c_{w,air}\text{-}c_{w,sat}(T_{wb})} = \frac{T_{air}\text{-}T_{surf}}{T_{air}\text{-}T_{wb}} \tag{25}$$

The saturated water vapor concentration is obtained from the ideal gas law and Clausius-Clapeyron relation (Çengel et al., 2015):

$$c_{w,sat}\left(T_{surf}\right) = \frac{P_{sat}^{T_{surf}}\, M_w}{R\, T_{surf}} \tag{26}$$

wherein $P_{sat}^{T_{surf}}$ is the saturated vapor pressure at a temperature T and R is the gas constant (8.314 J K^{-1} mol^{-1}). The water concentration at the surface was estimated through a GAB model for parameters $X_{w,mono}$, C and K resulting from desorption measurements.

In summary:

a) pilot-scale drying experiments allowed the monitoring of water content X_w and slice dimensions D and H under controlled ambient conditions;

b) for each of these ambient conditions, desorption models enabled us to estimate the equilibrium moisture X_{we} value;

c) with the latter, the evolution of the moisture ratio MR was represented through the two-parameter drying kinetics, providing the initial drying rate;

d) monitoring the slice dimensions allowed us to identify a mean shrinkage behavior, and hence to predict the slice surface evolution;

e) finally, the availability of water content and surface evolutions allowed us to estimate the surface temperature and the surface water activity (Eq. 25).

3.5 Statistical analyses

Vapor sorption isotherm data were fitted using nonlinear regression, through the Statgraphics Centurion XV software (StatPoint, Inc., USA). The agreement between the experimental data and the calculated values was assessed by the coefficient of determination (r^2) and root-mean-square error (RMSE).

Drying kinetics data were fitted using nonlinear regression, using the Solver tool from Excel 2019 (Microsoft, USA), and the agreement between experimental and model values was evaluated using the root mean square error (RMSE). The model parameters (eq. 13) were analyzed by the ANOVA applying Tukey's test at a 95% confidence level as a posthoc test, using Statgraphics Centurion XV software (StatPoint, Inc., USA).

4. Results

4.1. Vapor sorption isotherms

Vapor sorption isotherms for yacón (Fig. 2) can be characterized as being type III, which are common for products with a high quantity of soluble sugars (Rizvi, 2005; Al-Muhtaseb et al., 2002). It can be observed that there was little difference between static and dynamic methods, and between tested temperatures, and no visible hysteresis.

GAB model parameters, adjusted to the isotherms, are shown in Table 3. $X_{w,mono}$ is an estimation of the monolayer water content; under this value, food materials tend to be very stable (Roos, 2008). However, packaging conditions are important to delay the re-absorption of water.

4.2. Drying kinetics

Figure 3 shows the evolution of the moisture ratio of ensembles of yacón slices, under the ambient conditions here considered. Table 4 summarizes the results obtained after applying Eq.13, and other models available in the literature, to the data obtained from each of the three tests, carried out under each of the four controlled conditions. ANOVA performed along with an analysis of residuals, showed no evidence of heteroscedasticity in any of the tested models (Table 4). Some findings emerge from these results.

a) Under the ambient conditions considered, the application of Eq. 13 allows a smaller root-mean-square-error (RMSE) than other two-parameters models available in the literature. We argue that Eq. 13 constitutes a good option for engineering aims.
b) The influence of ambient conditions on the values estimated for model parameters is here preliminarily assessed because only three runs were conducted under each ambient condition. Excepting the Page model, the influence of both air temperature and relative humidity on parameter k_1 seems significant. This finding is consistent

with the physical meaning of this parameter; it is directly related to the initial drying rate, and its value increases with the driving force ($T_{air} - T_{wb}$). The influence of air temperature on the second parameter of Eq. 13, of Modified Page, and Henderson-Pabis models seems significant.

c) It is quite hard to compare model parameters estimated from our experimental data with those provided by other authors. Airflow and temperature conditions were different, and there was no control of air relative humidity, allowing ambient conditions which be perhaps unsteady. An additional difficulty comes from the diversity of yacón; Hermann et al. (1999) studied nine different cultivars of yacón, and they differed in appearance and composition: the dry matter content alone could range from 98 to 136 g/kg, suggesting that the drying kinetics can vary from a cultivar to another. Reis et al. (2012) reported the time of purchase, but not the location; Shi et al (2013) purchased their roots in China, and Lisboa et al. (2018) reported a purchase in Brazil, but not the season. None of these studies reported the variety used, nor any descriptors, there thus being a possibility that those authors studied different varieties of yacón.

4.3. Shrinkage

The left-hand side of Fig. 4 summarizes all the available experimental data, in terms of dimensionless values for the slice height (Fig. 4a) and diameter (4c) as a function of the dimensionless water content. Triplicates were conducted. The right-hand side of Fig. 4 compares measurements with similar predicted by hypothetical shrinkage behaviors; in the case of slice height, triangles indicate averaged values; in the case of slice diameter, measurements do not correspond to the same water content and then averaging was not possible.

Figures 4b and 4d compare measurements and hypothetical shrinkage behaviors: purely-vertical, isotropic and combined models for both diameter and height (Eqs. 8, 9, and 10, respectively). Up to X_w^* = 0.2, the slice diameter remained at more than 90 % of the initial value; the proposed vertical model is thus a more realistic approach than the isotropic one. Afterward, there was a drastic reduction in diameter. Figures 4b and 4d suggest that the combined behavior, which mixes the vertical and the isotropic approaches, describes the slice shrinkage better than the others. Looking for a consistent approach for predicting the shrinkage of yacón slices under convective drying, the combined approach was considered.

4.4. Heat transfer coefficient between yacón samples and surrounding air

A first estimation of the heat transfer coefficient relevant to our problem comes from experimental work with aluminum slices (sub-section 3.3.1). The results obtained were h = 41 W m^{-2} K^{-1} for the 35 mm cylinder and 53 W m^{-2} K^{-1} for the 20 mm one.

The consistency of these findings can be discussed using the correlation method. Taking into account uniform heat flux conditions over a flat plate under laminar flow, it can be shown that the averaged Nusselt, Reynolds and Prandtl numbers are related through the correlation $\mathrm{Nu} = \propto Re^{\beta} Pr^{\gamma}$ (Incropera et al., 2007, p.410). In our case, this expression can be rewritten to indicate the heat transfer coefficient as a function of the cylinder diameter: $h = \delta D^{\beta-1}$ wherein $\beta - 1 < 0$. According to this rationale, the heat transfer coefficient should increase during drying while the yacón dimension reduces. Hence, it is consistent to reach h = 41 W m^{-2} K^{-1} for experimental data collected with a 35 mm aluminum cylinder and 53 W m^{-2} K^{-1} with a 20 mm one.

A second estimation of the heat transfer coefficient between yacón samples and surrounding air can be obtained by applying the expression $h = \delta D^{\beta-1}$ to our experimental conditions. Given the airflow and temperature conditions above the surface of the cylinders, we can

estimate the Reynolds number to be about 10000 for a 40 mm cylinder (yacón sample, before any drying), hence lower than the critical value for the laminar-turbulent transition for external flow (Incropera et al., 2007, p.361). For these conditions, that correlation yields a heat transfer convective coefficient 39 $Wm^{-2}K^{-1}$ for a 40 mm cylinder. Note that the aforementioned correlation and the experimental values correspond to a physical problem bounded by an adiabatic surface below the cylinder.

Finally, the heat transfer coefficient between yacón samples and surrounding air was estimated by applying Eq. 20, i.e. by considering the initial evaporative rate results. The value obtained (32 W m^{-2} K^{-1}) implicitly takes into account the global influence of many factors affecting the heat and mass transfer relevant to the problem, including: a) the fact that not one but an ensemble of 42 yacón slices were simultaneously processed in the convective dryer pilot unit; b) the role played by the heterogeneous exposure of slices to airflow, c) the influence of thermal radiation interaction of slices with the metallic walls of the dryer, and d) the fact that there was a metallic holed surface below the yacón samples, allowing a complex situation of heat and mass transfer.

4.5. Predictions of temperature and water activity on the surface

Experimental results displayed in Fig. 3 suggest that the most reproducible condition was T_{air} = 60 °C, *RH* = 20 %. We hypothesize that better reproducibility is due to the humidity stabilization system of the convective dryer pilot unit. On the one hand, when the thermo-hygrometer detects a value of *RH* below the set point, the control system of the drying oven sprays water into the airflow and as it is not preheated, it could destabilize the temperature in the oven. On the other hand, when humidity is above the set point, the air passes through a refrigerating system, where water condensates and is removed, and the air must be heated again before re-entering the oven. At the highest temperature (60 °C), the air has a higher ability to hold water from the samples without going over the set point; and, in the lowest *RH*,

there is no need to add moisture to the air at the end of the drying process, to keep a high *RH*, leading to less destabilization. In the forthcoming last steps of this study, we restrict our attention to measurements and predictions corresponding to the ambient condition T_{air} = 60 °C, *RH* = 20%.

The identification of a suitable shrinkage behavior allows predicting the slice surface, which is exposed to surrounding air along the drying period (*S**). Representing the drying kinetics through the two-parameter model allows to predict, also along the whole period, the drying rate $\frac{dX_w^*}{dt^*}$. Figure 5a shows the predictions for the slice surface (Eq. 7) and the drying rate (Eqs. 14 and 22) as a function of the dimensionless water content. The influence of the total surface decrease on the drying rate $\frac{dX_w^*}{dt^* S^*}$ is noticeable, but only partially explains the drop in this drying rate. Figure 5b exhibits the same variables as a function of time, which can be compared with the classical drying curves (Mujumdar, 2006). Note that $\frac{dX_w^*}{dt^* S^*}$ does not present a constant rate period, indicating that some drying limitations due to the resistance of water migration from the center to the surface of the product may exist.

The availability of key quantities *S** and $\frac{dX_w^*}{dt^*}$ enables to estimate surface-averaged values for the temperature *T*, the water activity a_w and the water content X_w at the slice surface along the drying period. Figure 5c shows that, as expected, the predicted water content at the surface decreases more rapidly than the volume-averaged value for the sample. Note that GAB models do not accurately represent the sorption phenomena at very high (a_w > 0.93) water activities (Basu et al., 2006); hence, the predicted water content at the surface tends to be underestimated at the beginning of drying.

Finally, Fig. 5d displays the water activity and temperature at the product surface. In the case of the water activity, the departure from pre-drying conditions is immediate, contrarily to

451 experimental results (see for instance Figure 1 of Bernstein and Norena, 2014). In the case of
452 temperature, firstly the surface-averaged temperature increases almost instantaneously from
453 the initial product temperature (20 °C) up to the wet-bulb temperature (about 35 °C); later on,
454 this temperature increases from the wet-bulb temperature up to the air temperature along the
455 remaining drying period. It would be interesting to assess the reliability of these predictions,
456 for instance using a non-invasive technique, such as an infrared thermometer.

457 *4.6. A remark about moisture diffusivity*

458 Shi et al. (2013) and Lisboa et al. (2018) used the Crank (1975) solutions to Fick's laws to
459 estimate the effective moisture diffusion coefficient for yacón samples. These solutions,
460 however, assume that the shrinkage is negligible. Results in Section 4.3 demonstrate that this
461 is not the case for yacón samples as tested here. The infinite slab and the finite cylinder
462 models, common in the literature, revealed to be unreliable fits for the experimental drying
463 data displayed in Fig. 3. In the case of the infinite slab model, estimated moisture diffusivity
464 was 4.0 10^{-10} m^2 s^{-1} at 50 °C, and 7.4 10^{-10} m^2 s^{-1} at 60 °C, and a root mean square error of
465 0.033 and 0.060 in *MR* units, respectively. However, the fitted curve tended to underestimate
466 the moisture ratio at the beginning of the drying period and to overestimate it after two hours
467 of drying. Anyway, given the drastic differences in the sample's water content, dimensions
468 and temperature between the beginning and the end of the drying process, it is likely incorrect
469 to attribute a single, constant moisture diffusivity value over the whole drying process.

470 **5. Conclusions and Recommendations**

471 The study focused on the evolution of yacón samples having a particular shape and being
472 exposed to convective drying under controlled ambient conditions (mean air velocity of 4 m/s,
473 air temperature of 50 and 60 °C, air relative humidity of 20 and 30 %). The slice dimensions
474 were measured along the drying period, as an original contribution to the classical monitoring
475 of moisture loss. A dataset including triplicates of samples' water content, diameter and

476 height allowed us to study the evolution of yacón slices while including the influence of
477 shrinkage. Surface-averaged temperature and water activity tendencies were estimated from
478 standard assumptions about heat and mass transfer phenomena, providing a useful insight
479 about the drying evolution of a complex food product. The following conclusions were
480 reached.
481 i) The diameter of yacón slices decreased to about 60-70 % of the initial value after 6 hours
482 of drying without a clear dependence on the ambient condition under consideration, i.e.
483 following nearly the same decreasing tendency. The height of yacón slices was more difficult
484 to determine because of irregularities that progressively appeared on upper and lower surfaces
485 along the drying period. Available results indicated a reduction to 5-30 % of the initial value
486 after 6 hours of drying, with the decreasing tendency being faster in the samples dried at 20%
487 than in the samples dried at 30%, which can be explained by the faster dehydration if
488 Equations 10 and 11 are considered.
489 ii) In the case of yacón slices as tested here, a combined shrinkage behavior was identified: it
490 mixes purely-vertical (no diameter modification) with isotropic shrinkage (that progressively
491 operates inside the product matrix). Such a novel approach was later applied in predicting
492 firstly the slice total surface as a function of the water content inside it, and secondly the
493 evolution of selected properties at the yacón slice surface along the drying period.
494 iii) The application of a two-parameter model for representing the drying kinetics (Eq. 13)
495 allowed us to estimate the heat transfer coefficient between yacón samples and surrounding
496 ambient conditions. The value obtained (32 W m^{-2} K^{-1}) implicitly includes the global
497 influence of many factors affecting the heat and mass transfer relevant to the problem. Two
498 other approaches (experimental work with aluminum cylinders, and correlation involving
499 dimensionless numbers) provided independent estimates of this transfer coefficient, and the
500 whole set of results seems consistent.

iv) Evolutions of moisture ratio from measurements were poorly represented by the semi-theoretical model proposed by Lewis (1921), towards the ending of the drying period (Fig. 3). That classical model was proposed under some assumptions including negligible shrinkage, which constitutes a hypothesis unacceptable for yacón samples. The inclusion of a quadratic term in Eq. 13 mitigates this problem (Fig. 3). We argue that Eq. 13 constitutes a good option for engineering aims, in which the whole drying period must be represented as properly as possible.

v) The results from the energy balance allowed to estimate properties that could not be directly measured, or that would disturb the system. It gave insight on aspects that were not clear from the experimental data, such as the immediate decrease in the water activity and the different evolution of the water content on the sample surface and center.

The crucial issue of this study was to follow the dimensions of the sample throughout the drying period. Our pioneering strategy could be improved, for example by measuring the height of the sample using an optical detection method.

The suitability of our approach to the design and optimization of the process as well as of the final product could be explored. As a preliminary step, testing this approach should consider wider ranges of ambient conditions (airflow, temperature and relative humidity) and include different varieties of yacón and other raw food products. Much work remains to be done to clarify the relationship between shrinkage and moisture loss.

ACKNOWLEDGMENTS

The authors have received grants from the São Paulo Research Foundation (FAPESP), grants 2018/21327-1 and 2019/21832-0; from the Coordination for the Improvement of Higher Education Personnel - Brazil (CAPES) - Finance Code 001; and from the National Council for Scientific and Technological Development (CNPq), grant 306414/2017-1. We would like to thank AgroParistech and UMR Sayfood for receiving the first author for a one-year research internship abroad; and Emmanuel Bernuau, for his valuable help to calculate the heat transfer coefficient.

Declarations of interest: none.

REFERENCES

Al-Muhtaseb, A. H., McMinn, W. A. M., & Magee, T. R. A. (2002). Moisture sorption isotherm characteristics of food products: A review. *Food Bioproducts Process*, *80*, 118–128. https://doi.org/10.1205/09603080252938753.

AOAC. (1996). Moisture and volatile matter in oils and fats (926.12-1926). In *Official Methods of Analysis, 15th ed.*, Association of Official Analytical Chemists, Washington, USA.

Asioli, D., Aschemann-Witzel, J., Caputo, V., Vecchio, R., Annunziata, A., Næs, T., & Varela, P. (2017). Making sense of the "clean label" trends: A review of consumer food choice behavior and discussion of industry implications. *Food Research International, 99,* 58–71. https://doi.org/10.1016/j.foodres.2017.07.022.

Assis, F. R., Rodrigues, L. G. G., Tribuzi, G., de Souza, P. G., Carciofi, B. A. M., & Laurindo, J. B. (2019). Fortified apple (*Malus* spp., var. Fuji) snacks by vacuum impregnation of calcium lactate and convective drying. *LWT – Food Science and Technology, 113*, 108298. https://doi.org/10.1016/j.lwt.2019.108298.

544 Basu, S., Shivhare, U. S., & Mujumdar, A. S. (2006). Models for sorption isotherms for
545 foods: A review. *Drying Technology, 24*, 917–930.
546 https://doi.org/10.1080/07373930600775979.
547 * Bernstein, A., & Noreña, C. P. Z. (2014). Study of thermodynamic, structural, and quality
548 properties of yacón (*Smallanthus sonchifolius*) during drying. *Food and Bioprocess*
549 *Technology, 7*, 148-160. https://link.springer.com/article/10.1007/s11947-012-1027-y.
550 Blahovec, J., Lahodova, M., Kindl, M., & Fernandez, E. C. (2013). DMA thermal analysis of
551 yacón tuberous roots. *International Agrophysics, 27*, 479-483. https://doi.org/10.2478/intag-
552 2013-0018.
553 Campos, D., Aguilar-Galvez, A., & Pedreschi, R. (2016). Stability of fructooligosaccharides,
554 sugars and colour of yacón (*Smallanthus sonchifolius*) roots during blanching and drying.
555 *International Journal of Food Science and Technology*, *51*, 1177-1185.
556 https://doi.org/10.1111/ijfs.13074.
557 Çengel, Y., Boles, M., & Kanoğlu, M. (2015). Thermodynamic property relations. In:
558 *Thermodynamics an engineering approach*. Mc McGraw-Hill.
559 Castro, A. M., Mayorga, E. Y., & Moreno, F. L. (2018). Mathematical modelling of
560 convective drying of fruits: A review. *Journal of Food Engineering, 223*, 152-167.
561 https://doi.org/ 10.1016/j.jfoodeng.2017.12.012.
562 Choi, Y., & Okos, M. R. (1986). Effects of temperature and composition on the thermal
563 properties of foods. In M. Le Mageur, & P. Jelen (Eds.), *Food Engineering and Process*
564 *Applications* (pp. 93-101). Elsevier Applied Science.
565 Chua, K. J., Mujumdar, A. S., Chou, S. K., Hawlader, M. N. A., & Ho, J. C. (2000).
566 Convective drying of banana, guava and potato pieces : Effect of cyclical variations of air
567 temperature on drying kinetics and color change. *Drying Technology, 18*, 907–936.
568 https://doi.org/10.1080/07373930008917744.

569 Crank, J. (1975). *The Mathematics of Diffusion* (2nd ed.). Oxford University Press.
570 Curcio, S., & Aversa, M. (2014). Influence of shrinkage on convective drying of fresh
571 vegetables: A theoretical model. *Journal of Food Engineering, 123*, 36-49.
572 http://dx.doi.org/10.1016/j.jfoodeng.2013.09.014.
573 Fernández, E. C., Rajchl, A., Lachman, J., Čížková, H., Kvasnička, F., Kotíková, Z., &
574 Voldřich, M. (2013). Impact of yacón landraces cultivated in the Czech Republic and their
575 ploidy on the short- and long-chain fructo-oligosaccharides content in tuberous roots. *LWT -*
576 *Food Science and Technology, 54*, 80–86. https://doi.org/10.1016/j.lwt.2013.05.013.
577 Graefe, S., Hermann, M., Manrique, I., Golombek, S., & Buerkert, A. (2004). Effects of post-
578 harvest treatments on the carbohydrate composition of yacon roots in the Peruvian Andes.
579 *Field Crops Research, 86*, 157–165. https://doi.org/10.1016/j.fcr.2003.08.003.
580 Grau, A., & Rea, J. (1997). Yacón, Smallanthus sonchifolius (Poepp. et Endl.) H. Robinson.
581 In: M. Hermann & J. Heller (Eds.), *Promoting the conservation and use of underutilized and*
582 *neglected crops, #21, Andean roots and tubers: Ahipa, arracacha, maca and yacón* (pp. 199-
583 242). International Plant Genetic Resources Institute.
584 Hassini, L., Azzouz, S., Peczalski, R., & Belghith, A. (2007). Estimation of potato moisture
585 diffusivity from convective drying kinetics with correction for shrinkage. *Journal of food*
586 *engineering.* 79, 47–56. https://doi.org/10.1016/j.jfoodeng.2006.01.025.
587 * Hermann, M., Freire, I., & Pazos, C. (1999). Compositional diversity of the yacón storage
588 root. In *Andean Roots and Tuber Crops* (pp. 425-432). International Potato Center Program
589 Report 1997-1998.
590 Incropera, F. P., Witt, D. P., Bergman, T. L., Lavine, A. S. (2007). *Fundamentals of heat and*
591 *mass transfer* (6th ed.). Wiley, pp.253-263.
592 Khajehei, F., Hartung, J., & Graeff-Hönninger, S. (2018a). Total phenolic content and
593 antioxidant activity of yacón (*Smallanthus sonchifolius Poepp. and Endl.*) chips: Effect of

cultivar, pre-treatment, and drying. *Agriculture, 8*, 183. https://doi.org/10.3390/agriculture8120183.

Khajehei, F., Merkt, N., Claupein, W., & Graeff-Hönninger, S. (2018b). Yacón (*Smallanthus sonchifolius Poepp. & Endl.*) as a novel source of health promoting compounds: Antioxidant activity, phytochemicals and sugar content in flesh, peel, and whole tubers of seven cultivars. *Molecules, 23,* 278. http://dx.doi.org/10.3390/ molecules23020278.

Lachman, J., Fernández, E. C., & Orsák, M. (2003). Yacón [*Smallanthus sonchifolia (Poepp. et Endl.) H. Robinson*] chemical composition and use: A review. *Plant, Soil and Environment, 49*, 283–290. https://doi.org/10.17221/4126-PSE.

Lebeda, A., Doležalová, I., Fernández, E., & Viehmannová, I. (2012). Yacón (*Asteraceae*; *Smallanthus sonchifolius*). In R. J. Singh (Ed.), *Genetic Resources, Chromosome Engineering, and Crop Improvement. Volume 6: Medicinal Plants* (pp. 641-702). CRC Press.

* Lewis, W. K. (1921). The rate of drying of solid materials. *Industrial & Engineering Chemistry Research, 13*, 427–432. https://doi.org/10.1021/ie50137a021.

Lisboa, C., Gomes, J., Figueirêdo, R., Queiroz, A., Diógenes, A., & de Melo, J. (2018). Effective diffusivity in yacón potato cylinders during drying. *Revista Brasileira de Engenharia Agrícola e Ambiental, 22*, 564–569. https://doi.org/10.1590/1807-1929/agriambi.v22n8p564-569.

* Mayor, L., & Sereno, A. M. (2004). Modelling shrinkage during convective drying of food materials: A review. *Journal of Food Engineering, 61*, 373-386. http://dx.doi.org/10.1016/S0260-8774(03)00144-4.

McCabe, W., Smith, J., & Harriott, P. (2014). Drying of solids. In: *Unit operations of chemical engineering* (7th ed.). Mc Graw Hill.

617 Moreira, R., Figueiredo, A., & Sereno, A. (2000). Shrinkage of apple disks during drying by
618 warm air convection and freeze drying. *Drying Technology*, *18*, 279-294.
619 https://doi.org/10.1080/07373930008917704.
620 Mujumdar, A. S. (2006). Principles, Classification, and Selection of Dryers. In *Handbook of*
621 *Industrial Drying*. Taylor and Francis.
622 Panchariya, P. C., Popovic, D., & Sharma, A. L. (2002). Thin-layer modelling of black tea
623 drying process. *Journal of Food Engineering*, *52*, 349-357. https://doi.org/10.1016/S0260-
624 8774(01)00126-1.
625 Perussello, C. A., Mariani, V. C., Masson, M. L., & Castilhos, F. (2013). Determination of
626 thermophysical properties of yacón (*Smallanthus sonchifolius*) to be used in a finite element
627 simulation. *International Journal of Heat and Mass Transfer, 67*, 1163-1169.
628 http://dx.doi.org/10.1016/j.ijheatmasstransfer.2013.09.004.
629 Perussello, C. A., Kumar, C., De Castilhos, F., & Karim, M. A. (2014). Heat and mass
630 transfer modeling of the osmo-convective drying of yacón roots (*Smallanthus sonchifolius*).
631 *Applied Thermal Engineering*, *63*, 23–32.
632 https://doi.org/10.1016/j.applthermaleng.2013.10.020.
633 Perry, R. H., & Green, D. W. (1997). Section 2: Physical and chemical data. In *Perry's*
634 *Engineers' Handbook* (7th ed.). Mc Graw-Hill.
635 Rizvi, S. H. (2005). Thermodynamic Properties of Foods in Dehydration. In *Engineering*
636 *Properties of Foods* (3rd ed.). Boca Raton: CRC Press.
637 Reis, F. R., Lenzi, M. K., de Muñiz, G. I. B., Nisgoski, S., & Masson, M. L. (2012). Vacuum
638 drying kinetics of yacón (*Smallanthus sonchifolius*) and the effect of process conditions on
639 fractal dimension and rehydration capacity. *Drying Technology, 30*, 13–19.
640 https://doi.org/10.1080/07373937.2011.611307.

641 Roos, Y.H. (2008). Water Activity and Glass Transition. In *Water Activity in Foods:*
642 *Fundamentals and Applications*, (1st ed.). Blackwell Publishing Professional.
643 * Scher, C. F., Rios, A., & Noreña, C. (2009). Hot air drying of yacón (*Smallanthus*
644 *sonchifolius*) and its effect on sugar concentrations. *International Journal of Food Science*
645 *and Technology, 44*, 2169–2175. https://doi.org/10.1111/j.1365-2621.2009.02056.x.
646 Salinas, J. G., Alvarado, J. A., Bergenståhl, B., & Tornberg, E. (2018). The influence of
647 convection drying on the physicochemical properties of yacón (*Smallanthus sonchifolius*).
648 *Heat and Mass Transfer, 54*, 2951-2961. https://doi.org/10.1007/s00231-018-2334-2.
649 Sandoval-Torres, S., Tovilla-Morales, A. S., & Hernández-Bautista, E. (2017). Dimensionless
650 modeling for convective drying of tuberous crop (Solanum tuberosum) by considering
651 shrinkage. *Journal of Food Engineering, 214*, 147–157.
652 https://doi.org/10.1016/j.jfoodeng.2017.06.014.
653 Seminario, J., Valderrama, M., & Manrique, I. (2003). *El Yacón : Fundamentos para el*
654 *Aprovechamiento de un Recurso Promisorio*. Lima (Peru): Centro Internacional de la Papa
655 (CIP), Universidad Nacional de Cajamarca, Agencia Suiza para el Desarollo y la Cooperacion
656 (COSUDE).
657 Shi, Q., Zheng, Y., & Zhao, Y. (2013). Mathematical modeling on thin-layer heat pump
658 drying of yacón (*Smallanthus sonchifolius*) slices. *Energy Conversion and Management, 71*,
659 208–216. https://doi.org/10.1016/j.enconman.2013.03.032.
660 Shi, Q., Zheng, Y., & Zhao, Y. (2015). Thermal transition and state diagram of yacón dried
661 by combined heat pump and microwave method. *Journal of Thermal Analysis and*
662 *Calorimetry, 119*, 727–735. https://doi.org/10.1007/s10973-014-4198-0.
663 Sjoholm, I., & Gekas, V. (1995). Apple shrinkage upon drying. *Journal of Food Engineering,*
664 *25*, 123-130. https://doi.org/10.1016/0260-8774(94)00001-P.

665 Suzuki, K., Kubota, K., Hasegawa, T., & Hosaka, H. (1976). Shrinkage in dehydration of root
666 vegetables. *Journal of Food Science, 41,* 1189–1193. https://doi.org/10.1111/j.1365-
667 2621.1976.tb14414.x.
668 van den Berg, C. (1984). Description of water activity of foods for engineering purposes by
669 means of the G.A.B. model of sorption. In B. M. McKenna (Ed.), *Engineering and Food*
670 *(Proceedings of the Third International Congress on Engineering and Food held between 26*
671 *and 28 September 1983 at Trinity College, Dublin, Ireland)* (vol. 1, pp. 311-321). London
672 (UK): Elsevier Applied Science Publishers.
673 Watzl, B., Girrbach, S., & Roller, M. (2005). Inulin, oligofructose and immunomodulation.
674 *British Journal of Nutrition, 93,* S49. https://doi.org/10.1079/BJN20041357.
675 Yan, X., Suzuki, M., Ohnishi-Kameyama, M., Sada, Y., Nakanishi, T., & Nagata, T. (1999).
676 Extraction and identification of antioxidants in the roots of yacón (*Smallanthus sonchifolius*).
677 *Journal of Agricultural and Food Chemistry, 47,* 4711–4713.
678 https://doi.org/10.1021/jf981305o.

679 **Figure captions**

680 **Fig. 1.** Yacón roots: (a) in *natura*, still with their tan-colored peel; (b) being cut for the drying
681 experiments, with their light-yellow flesh visible; (c) dried, with the perforated tray on the
682 background; and (d) experimental arrangement to estimate the heat transfer coefficient.

683 **Fig. 2.** Sorption isotherms (desorption and adsorption) for yacón obtained at two temperatures
684 through the methods DDI and DVS, in comparison with the adjusted GAB model for DVS
685 test at 60 °C.

686 **Fig. 3.** Moisture ratio of yacón slices, expressed in function of time (a) at T_{air} = 50 °C and *RH*
687 = 30 %; (b) at 60 °C and 30 %; (c) at 50 °C and 20 %; (d) at 60 °C and 20 %, compared to the
688 drying kinetics model proposed in this work, and to the Lewis (1921) model.

689 **Fig. 4.** Dimensionless height and diameter of yacón slices as a function of dimensionless
690 water content along with the drying: (a) all height measurements performed under four
691 ambient conditions; (b) height measurement averages, compared to predictions reached after
692 assuming different hypothetical behaviors for slice shrinkage; (c) as in (a) but for the
693 diameter; (d) as in (b) but for the diameter. In the case of the vertical shrinkage assumption,
694 the dimensionless diameter equals unity (Eq.8).

695 **Fig. 5.** Predictions about the drying behavior of yacón slices. In-display (a), the dimensionless
696 surface S^* comes from Eq.7, the drying rate dX_w^*/dt^* comes from Eq.22 with dMR/dt
697 from Eq.14. In-display (b), same as (a) but as a function of time. In-display (c), slice-averaged
698 and surface moisture as a function of time. In-display (d), surface temperature from Eq.21 and
699 water activity from Eq.25 as a function of time.

Justifying key references

Please see below our remarks regarding our five key references, sorted by year of publication. They are indicated by a star in the reference section of our manuscript.

1) Lewis, W. K. - 1921 - The rate of drying the solid materials. The Journal of Industrial and Engineering Chemistry, 13: 427-432. https://doi.org/10.1021/ ie50137a021.

> This founding article allowed us to understand the basic rationale of semi-theoretical drying kinetics models. The Lewis' model can be presented as

$$d\,MR / dt = -k\,t,$$

where symbols are explained in our Nomenclature. In the present study we propose an extension of the Lewis' model:

$$d\,MR / dt = -k_1\,t - k_2\,t^2.$$

The second-order term might incorporate, implicitly, the bulk influence of complex phenomena in drying the solid matrix (including shrinkage, which was neglected by Lewis). Results suggest that this extended model fits better our experimental data than Lewis' one.

2) Hermann, M., Freire, I., Pazos, C. - 1999 - Compositional diversity of the yacón storage root. In « Andean Roots and Tuber Crops », International Potato Center Program Report 1997-1998, Lima (Peru), pp.425-432.

> Very few articles compare the physicochemical composition (fibers, proteins, carbohydrates, etc) of different yacón varieties. This article allowed us to estimate the dry-matter mass density associated with an averaged composition over nine yacón cultivars.

3) Mayor, L., Sereno, A. M. - 2004 - Modelling shrinkage during convective drying of food materials: A review. Journal of Food Engineering, 61: 373-386. https://doi.org/10.1016/S0260-8774(03)00144-4.

723 > This classical reference inspired us in our analysis of experimental data, more precisely in
724 comparing measurements of dimensions of yacón slices along the drying period with
725 predictions from hypothetical shrinkage behaviors.
726 4) Scher, C. F., Rios, A. O., Norena, C. P. Z. - 2009 - Hot air drying of yacón (Smallanthus
727 sonchifolius) and its effect on sugar concentrations. International Journal of Food Science and
728 Technology, 44: 2169-2175. https://doi.org/10.1111/j.1365-2621.2009.02056.
729 > This dense article discusses the influence of drying conditions on yacón sugar contents and
730 water activity, among other relevant characteristics. The design of our experimental work was,
731 to some extent, inspired by this article.
732 5) Bernstein, A., Norena, C. P. Z. - 2014 – Study of thermodynamic, structural, and quality
733 properties of yacón (Smallanthus sonchifolius) during drying. Food and Bioprocess
734 Technology, 7: 148-160. https://link.springer.com/article/ 10.1007/s11947-012-1027-y.
735 > This very interesting article provided us insight about yacón samples: their volume reduction
736 along some hours of drying, their micro-structure after different treatments, and water activity
737 at selected temperatures.

NOMENCLATURE

a_w	Water activity [-]
$a_{w,\mathrm{surf}}$	Water activity at the slice surfaces [-]
b	Moisture-dependent weighting parameter [-]
C	Guggenheim constant, GAB model [-]
C_P	Specific heat [J $kg^{-1}K^{-1}$]
$c_{w,\mathrm{air}}$	Water vapor concentration in the surrounding air [kg m^{-3}]
$c_{w,\mathrm{sat}}\,(T)$	Concentration of water in saturated air at a temperature T [kg m^{-3}]
$c_{w,\mathrm{surf}}$	Concentration of water vapor in the air at the surface of the product [kg m^{-3}]
D	Diameter [m]
D_0	Initial diameter of the food slice before drying [m]
D^*	Dimensionless diameter of the food slice (D/D_0)
D^*_{comb}	D^* assuming combined shrinkage behavior [-]
D^*_{iso}	D^* assuming isotropic shrinkage [-]
D^*_{vert}	D^* assuming vertical shrinkage only [-]
h	Heat transfer coefficient [$Wm^{-2}\,K^{-1}$]
H	Height [m]
H_0	Initial height of the food slice before drying [m]
H^*	Dimensionless height of the food slice (H/H_0)
H^*_{comb}	H^* assuming combined shrinkage behavior [-]
H^*_{iso}	H^* assuming isotropic shrinkage [-]
H^*_{vert}	H^* assuming vertical shrinkage only [-]
k	Convective mass transfer coefficient [m s^{-1}]

K	GAB correction factor [-]
k_1	Kinetic model parameter [s^{-1}]
k_2	Kinetic model parameter [s^{-1}]
L_v	Latent heat of evaporation of water [J kg^{-1}]
m	Mass [kg]
m_{dm}	Dry-matter mass [kg]
m_w	Water mass [kg]
MR	Moisture ratio [-]
M_w	Molar mass of water [g/mol]
Nu	Nusselt number [-]
P_{sat}^T	Saturated vapor pressure at a temperature T [Pa]
Pr	Prandtl number [-]
R	Gas constant, 8.314 [J K^{-1} mol^{-1}]
Re	Reynolds number [-]
S	Total surface of the food slice [m^2]
S_0	Initial total surface of the food slice before drying [m^2]
S^*	Dimensionless total surface of the slice
S_{comb}^*	S^* assuming combined shrinkage behavior [-]
t	Time [s]
t^*	Dimensionless time
T	Temperature [ºC]
T_{air}	Air temperature [°C]
T_{surf}	Temperature at the slice surface [°C]

T_{wb}	Wet-bulb temperature [°C]
V	Volume
V_0	Initial volume of the food slice before drying [m^3]
V^*	Normalized volume [-]
X_{we}	Estimated water content in the equilibrium, on dry basis [kg/kg]
X_w	Measured water content in the food product, on dry basis [kg/kg]
$X_{w,\text{mono}}$	Monolayer water content [kg/kg], dry basis
X_{w0}	Initial water content of the food product before drying [kg/kg], on dry basis
X_w^*	Dimensionless water content in the food product [-]
Greek letters	
α	Constant for Nusselt correlation [-]
β	Constant for Nusselt correlation [-]
γ	Constant for Nusselt correlation [-]
δ	Constant for Nusselt correlation [-]
λ	Thermal conductivity [$Wm^{-1}\ K^{-1}$]
ρ	Dry-matter mass density [kg m^{-3}]
ρ_{dm}	Dry-matter mass density [kg m^{-3}]
ρ_w	Water density [kg m^{-3}]

Table 1

Dimensions and thermophysical properties of the aluminum cylinders used to estimate the heat transfer coefficient.

Piece	1	2
D [mm]	35	20
H [mm]	7	3
Hole volume [m^3]	$7.07\ 10^{-8}$	$7.07\ 10^{-8}$
Cylinder volume [m^3]	$6.66\ 10^{-6}$	$0.87\ 10^{-6}$
Mass [g]	17.99	2.35
Surface area (A_S), exposed to airflow [m^2]	$1.7\ 10^{-3}$	$0.5\ 10^{-3}$
Thermophysical properties at 331 K*		
λ (W m^{-1} K^{-1})	238.0	
C_p (J kg^{-1} K^{-1})	917.6	
ρ (kg m^{-3})	2707	

*Source: Perry & Green (1997)

Table 2.

Models used in the literature to describe drying kinetics.

Model	Equation	Reference
Lewis	$MR = exp(-k_1\, t)$	Lewis (1921)
Page	$MR = exp(-k_1\, t^n)$	Panchariya et al. (2002); Shi et al. (2013)
Modified Page	$MR = exp(-k_1\, t)^n$	Panchariya et al. (2002); Shi et al. (2013)
Henderson-Pabis	$MR = a\, exp(-k_1\, t)$	Panchariya et al. (2002); Shi et al. (2013)

Table 3

GAB model parameters* adjusted to experimental data of yacón, for adsorption and desorption curves, through the dynamic (DDI) and static (DVS) operation modes.

	$X_{w,\text{mono}}$ [kg/kg, d.b.]		C [-]		K [-]	
Mode	adsorption	desorption	adsorption	desorption	adsorption	desorption
DDI 50 °C	$1.04\ 10^{-1}$	$1.29\ 10^{-1}$	$1.12\ 10^{0}$	$1.32\ 10^{0}$	$1.00\ 10^{0}$	$9.73\ 10^{-1}$
DDI 60 °C	$1.79\ 10^{-1}$	$1.34\ 10^{-1}$	$7.34\ 10^{-1}$	$2.06\ 10^{0}$	$9.41\ 10^{-1}$	$9.79\ 10^{-1}$
DVS 50 °C	$1.20\ 10^{-1}$	$1.37\ 10^{-1}$	$1.41\ 10^{0}$	$1.17\ 10^{0}$	$9.71\ 10^{-1}$	$9.70\ 10^{-1}$
DVS 60 °C	$1.21\ 10^{-1}$	$1.16\ 10^{-1}$	$9.08\ 10^{-1}$	$1.45\ 10^{0}$	$9.79\ 10^{-1}$	$9.84\ 10^{-1}$

*All adjustments had a Pearson's correlation coefficient higher than 0.997.

Table 4. Parameters for selected models, estimated from yacón drying kinetics; and comparison between this work and values from the literature. In the case of results from this work, values provided are indicated as arithmetic average ± standard deviation over triplicates.

Model		This work*				Reis *et al.* (2012)	Shi et al. (2013)	Lisboa *et al.* (2018)	
		T_{air} = 50 °C, RH = 30 % (T_{wb} = 32.6 °C), 4 m/s	T_{air} = 60 °C, RH = 30 % (T_{wb} = 40.0 °C), 4 m/s	T_{air} = 50 °C, RH = 20 % (T_{wb} = 28.7 °C), 4 m/s	T_{air} = 60 °C, RH = 20 % (T_{wb} = 35.4 °C), 4 m/s	T_{air} = 55 °C, 11.325 Pa**	T_{air} = 45°C, 1.5 m/s	T_{air} = 50 °C, 1.5 m/s	T_{air} = 60 °C, 1.5 m/s
Eq.13	k_1 [$\times 10^{-4}$ s^{-1}]	1.05 ± 0.004 ^{aA}	1.30 ± 0.09 ^{bB}	1.15 ± 0.03 ^{aA}	1.42 ± 0.04 ^{bB}				
	k_2 [$\times 10^{-5}$ s^{-1}]	5.94 ± 0.1 ^{aA}	6.88 ± 0.4 ^{bA}	5.40 ± 0.9 ^{aA}	6.08 ± 0.2 ^{bA}				
	RMSE	1.39×10^{-2}	1.85×10^{-2}	1.16×10^{-2}	8.00×10^{-3}				
Lewis	k_1 [$\times 10^{-4}$ s^{-1}]	1.37 ± 0.02 ^{aA}	1.75 ± 0.07 ^{bA}	1.42 ± 0.05 ^{aA}	1.72 ± 0.02 ^{bA}		1.18×10^{-4}		
	RMSE	3.42×10^{-2}	3.46×10^{-2}	2.58×10^{-2}	2.26×10^{-2}		3.38×10^{-2}		
Page	k_1 [$\times 10^{-5}$ s^{-1}]	2.52 ± 0.7 ^{aA}	3.03 ± 1 ^{aA}	3.83 ± 1 ^{aA}	4.21 ± 0.7 ^{aA}	3.83×10^{-5}	9.11×10^{-5}	3.03×10^{-5}	4.69×10^{-5}
	n [-]	1.19 ± 0.03 ^{aA}	1.20 ± 0.04 ^{aA}	1.15 ± 0.04 ^{aA}	1.20 ± 0.04 ^{aA}	1.50	1.24	0.95	1.90
	RMSE	1.16×10^{-1}	1.05×10^{-1}	1.09×10^{-1}	9.65×10^{-2}	R^2 = 0.995	1.45×10^{-2}	R^2 = 0.999	R^2 = 0.999
Modified Page	k_1 [$\times 10^{-4}$ s^{-1}]	1.33 ± 0.02 ^{aA}	1.60 ± 0.2 ^{bA}	1.39 ± 0.04 ^{aA}	1.64 ± 0.07 ^{bA}	7.42×10^{-5}	1.13×10^{-4}		
	n [-]	1.20 ± 0.02 ^{aA}	1.20 ± 0.04 ^{aA}	1.16 ± 0.05 ^{aA}	1.16 ± 0.02 ^{aA}	1.50	1.24		
	RMSE	1.91×10^{-2}	1.95×10^{-2}	1.56×10^{-2}	1.12×10^{-2}	R^2 = 0.995	1.47×10^{-2}		
Henderson-Pabis	k_1 [$\times 10^{-4}$ s^{-1}]	1.44 ± 0.04 ^{aA}	1.81 ± 0.2 ^{bA}	1.49 ± 0.09 ^{aA}	1.79 ± 0.07 ^{bA}	8.33×10^{-5}	1.24×10^{-4}	2.31×10^{-6}	2.81×10^{-6}
	a [-]	1.06 ± 0.01^{aA}	1.09 ± 0.02 ^{aA}	1.05 ± 0.03 ^{aA}	1.06 ± 0.01 ^{aA}	1.07	1.05	0.98	0.97
	RMSE	2.95×10^{-2}	2.90×10^{-2}	2.31 10^{-2}	1.91×10^{-2}	R^2 = 0.967	3.00×10^{-2}	R^2= 0.999	R^2= 0.999

*Same lower-case letters on the same line indicate no significant difference in relation to the temperature, and upper-case letters, in relation to the relative humidity (p > 0.05).
**Absolute pressure.

Figure

Click here to access/download;Figure;GraphicalAbstract.pptx

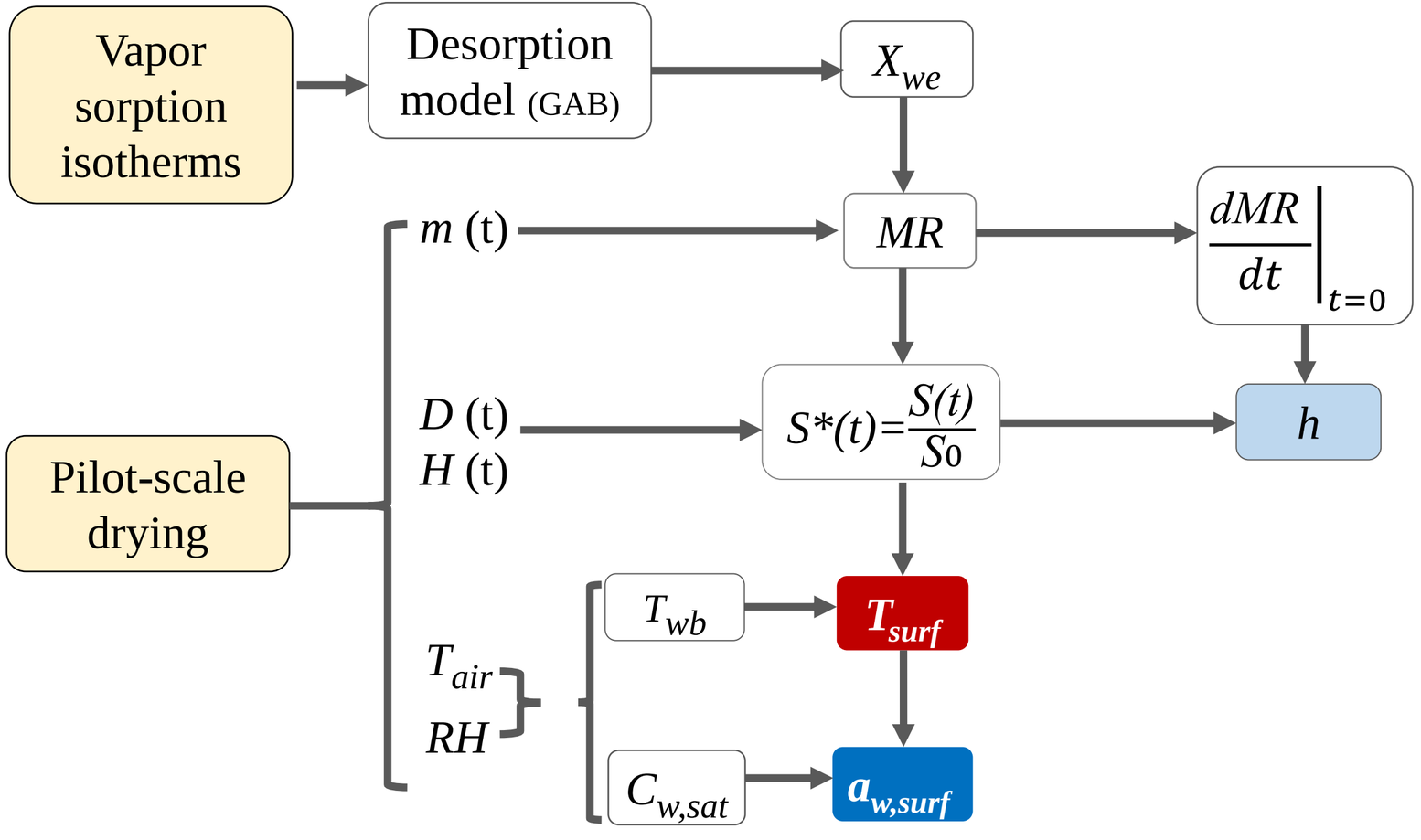

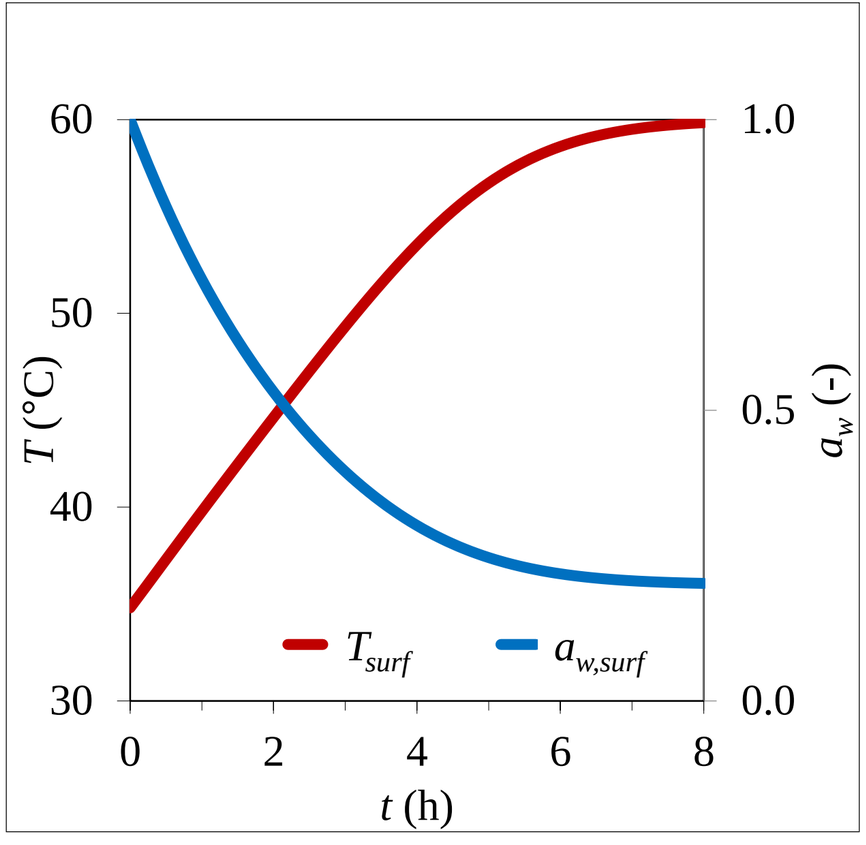

Figure

Click here to access/download;Figure;Figure1.pptx

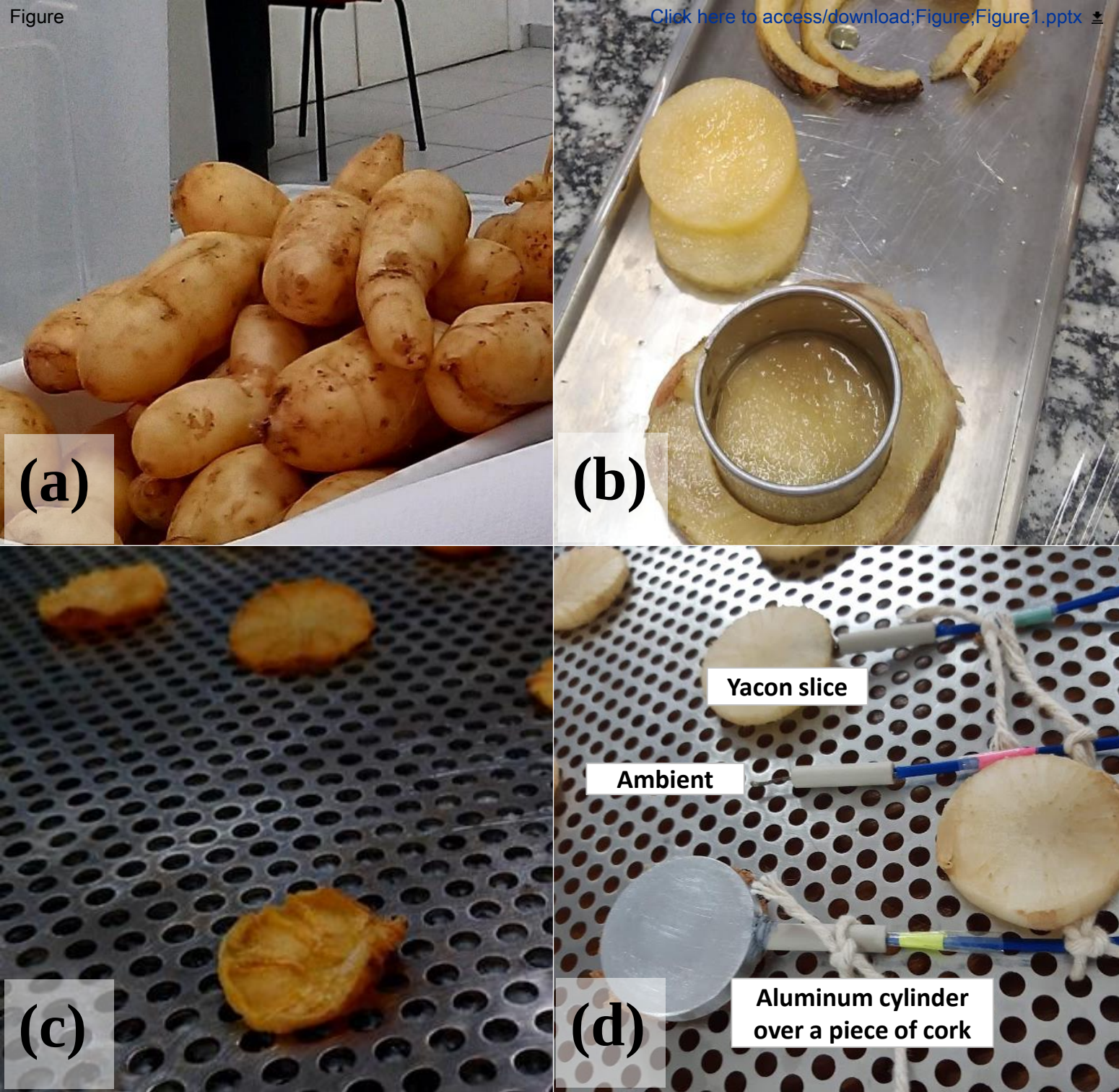

Figure

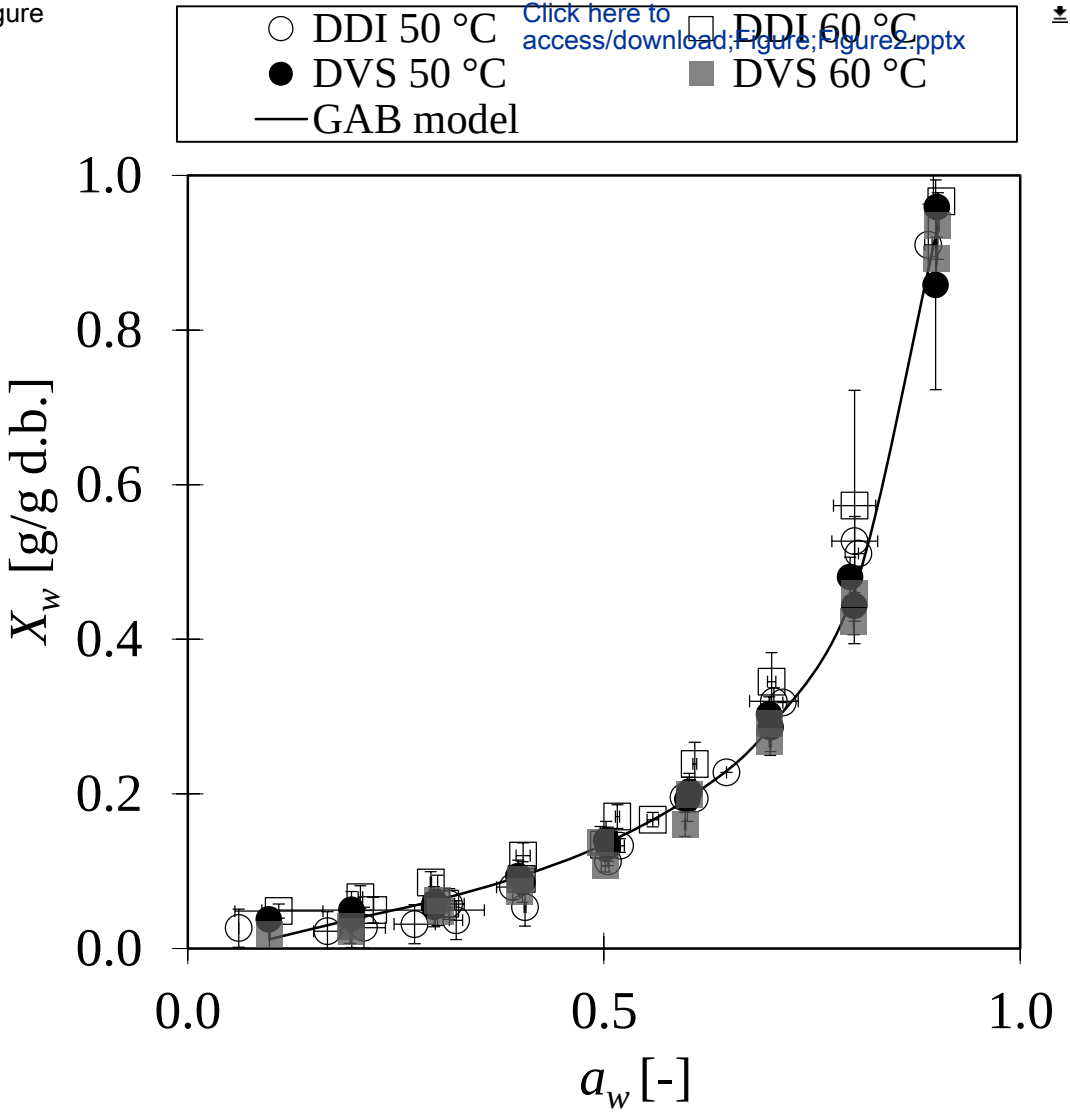

Figure

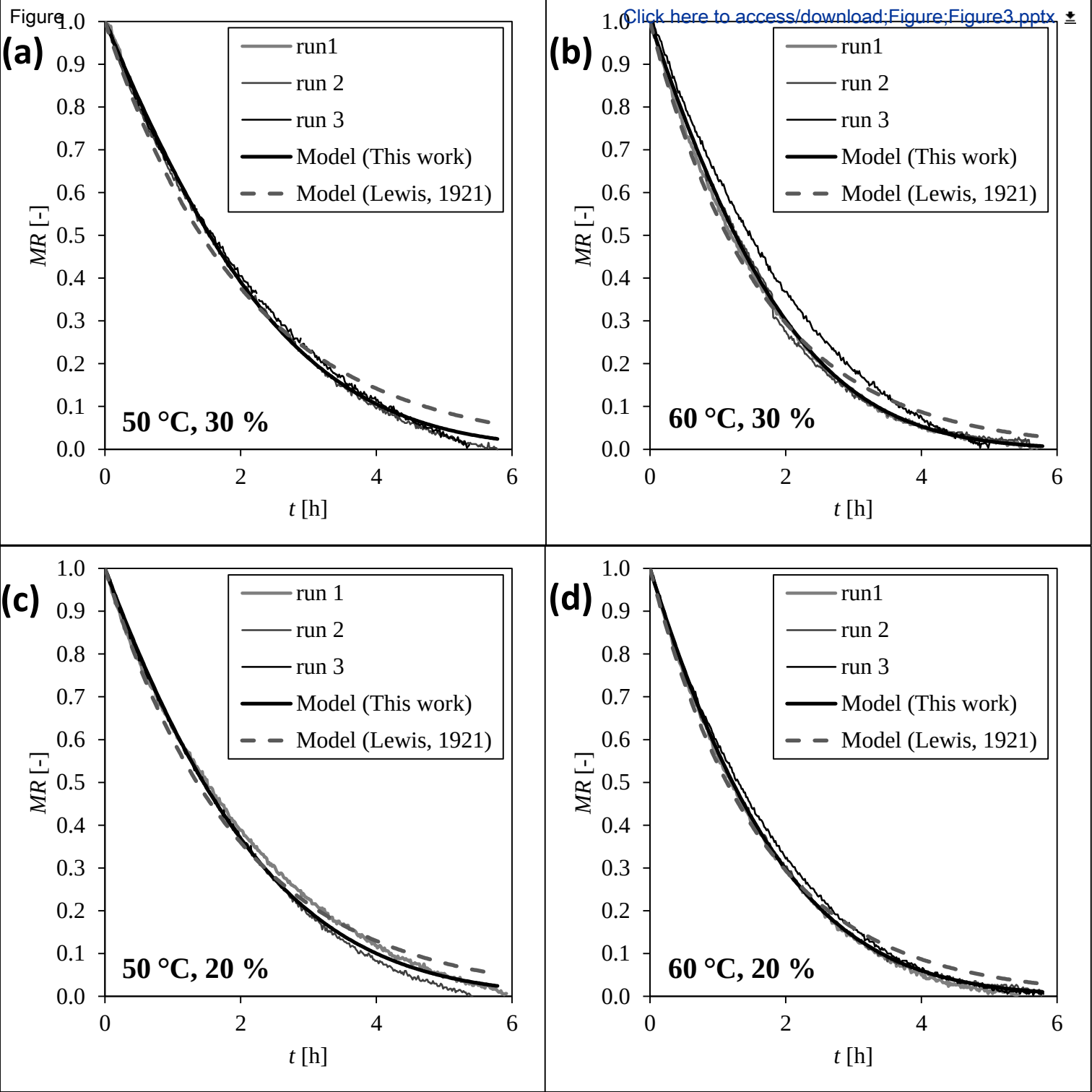

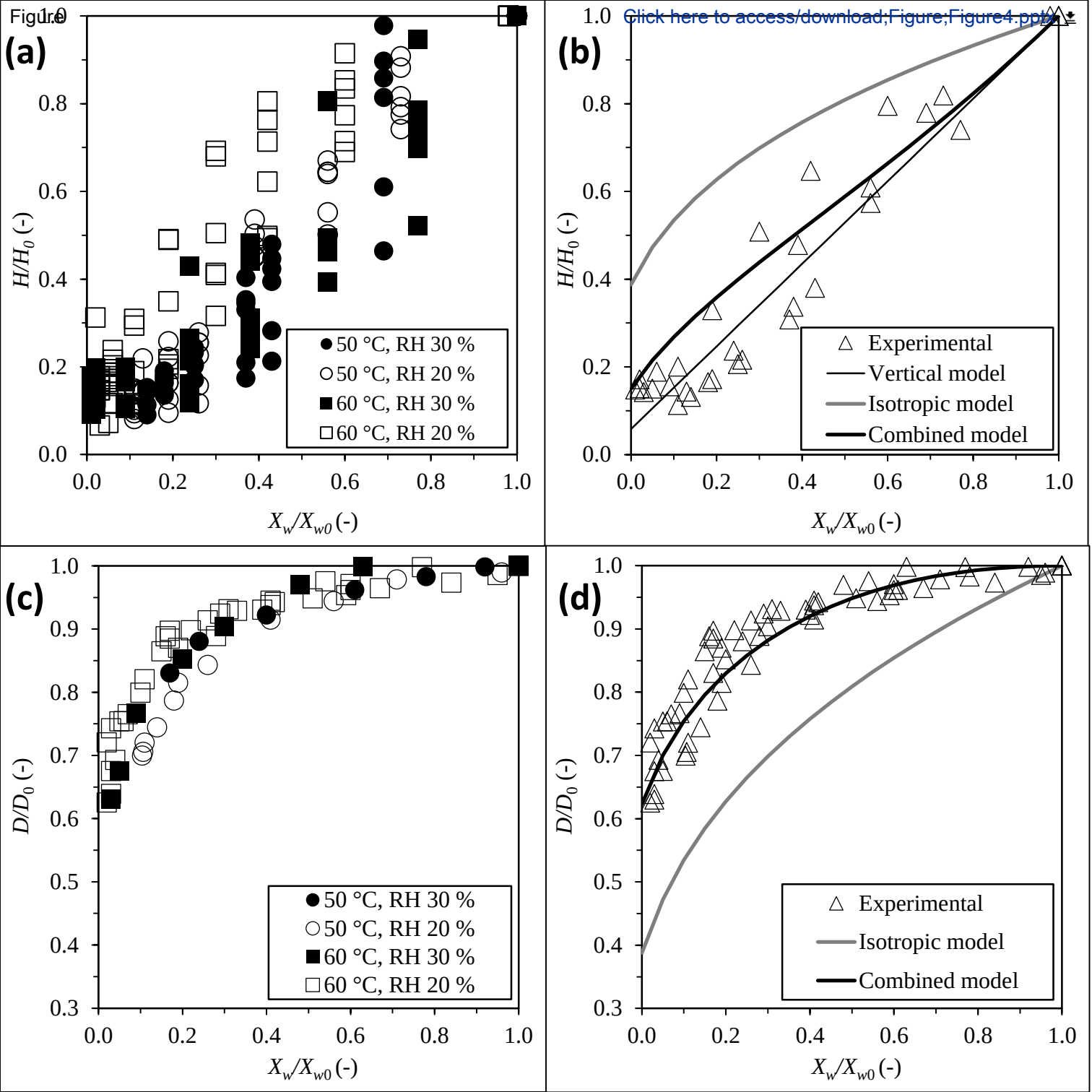

Figure

Click here to access/download;Figure;Figure5.pptx

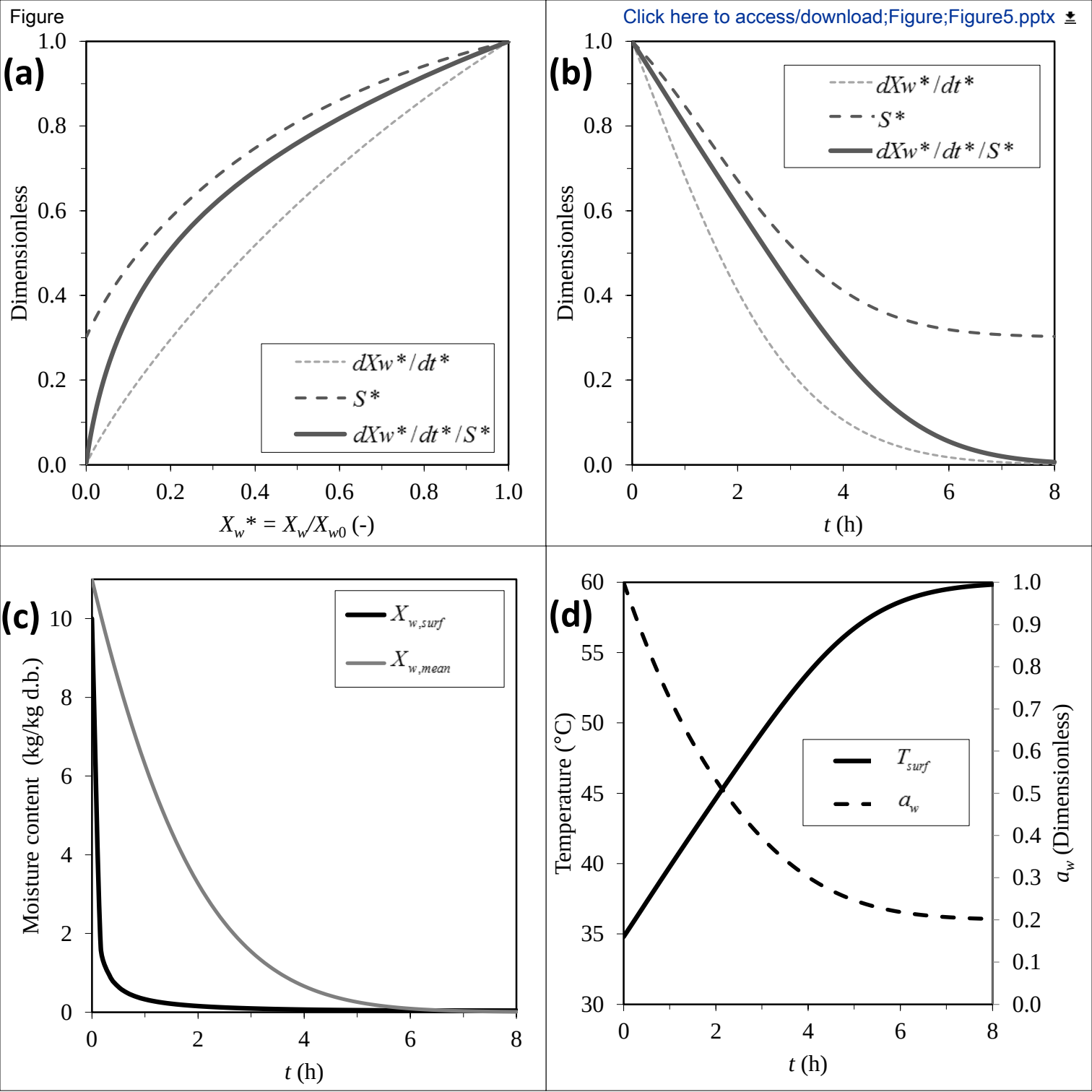

Conflict of Interest and Authorship Conformation Form

Please check the following as appropriate:

✓ All authors have participated in (a) conception and design, or analysis and interpretation of the data; (b) drafting the article or revising it critically for important intellectual content; and (c) approval of the final version.

✓ This manuscript has not been submitted to, nor is under review at, another journal or other publishing venue.

✓The authors have no affiliation with any organization with a direct or indirect financial interest in the subject matter discussed in the manuscript

- The following authors have affiliations with organizations with direct or indirect financial interest in the subject matter discussed in the manuscript:

Author's name	Affiliation
Artemio Plana-Fattori	Agro ParisTech
Bianca Cristine Marques	Universidade de São Paulo-USP
Carmen Cecilia Tadini	Universidade de São Paulo-USP
Denis Flick	Agro ParisTech

CREDIT AUTHOR STATEMENT

Bianca C. Marques: Methodology, Software, Formal analysis, Investigation, Resources, Writing-Original Draft, Writing-Review and Editing, Funding acquisition

Artemio Plana-Fattori: Methodology, Software, Formal analysis, Writing-Original Draft, Writing-Review and Editing, Project administration

Denis Flick: Conceptualization, Methodology, Software, Formal analysis

Carmen C. Tadini: Conceptualization, Formal analysis, Investigation, Resources, Writing-Review and Editing, Supervision, Project administration, Funding acquisition